AN EXPERIMENTAL METHOD FOR DETERMINATION OF POISSON'S RATIO IN SOILS

by

Julian Coronel-Ramirez

A Thesis Submitted to the
Graduate Faculty in Partial Fulfillment of
The Requirements for the Degree of
MASTER OF SCIENCE

Major Subject: Soil Engineering

Approved:

Robert A. Lohnes
In Charge of Major Work

Carl E Ebeling
Head of Major Department

J B Page 1x May
Dean of Graduate College

Iowa State University
Ames, Iowa

1969

TABLE OF CONTENTS

DEDICATION

This thesis is dedicated to my wife Patricia
and my beloved parents Jorge and Beatriz

ACKNOWLEDGMENTS

I wish to leave a written record of my everlasting gratitude to the Iowa State University Engineering Research Institute for having granted me the opportunity to pursue the academic studies I have made. Likewise, my deep gratitude and appreciation to all the honest dedicated professors for their delivered knowledge and guidance.

I thank specially to Dr. Robert A. Lohnes for his confidence in my work, the encouragement to search through new paths and his generous help. I equally thank Dr. Turgut Demirel and Professor William F. Riley for helpful discussions.

I am indebted to Mr. Rushell Fish and Mr. Kenneth Bergeson who found time in their busy schedules to write the computer program as well as to Mr. Darwin Fox for inking the presented charts.

I thank my wife, Patricia, for the special care she took to rear up our little daughters, and for softening these days with love and comprehension.

CHAPTER I: INTRODUCTION

Concepts

The theory of elasticity furnishes equations that tie together the stresses and displacements induced in an elastic body by the action of exterior causes. Its target is to determine the intensity and orientation of these stresses and displacements at any point. When a cylindrical elastic body is subjected to axial tension or compressions along the longitudinal axis, without lateral constraint, the elastic solution yields:

$$\frac{\partial \omega}{\partial z} = \varepsilon_{\ell} = \frac{\lambda + \mu}{2\mu^2 + 3\lambda\mu} \quad F$$

Where:

ω = vertical displacement

ε_{ℓ} = strain per unit of height

λ and μ = Lame's elastic constants. λ and μ are the only two independent constants that appear relating the stresses and strains in the general elastic equations.

μ is also called the shear modulus. It relates the shear stress to the shear strain through the expression: $T = \mu\gamma$

Where: T = shear stress

γ = shear strain

F = unit compressive or tensile force.

The coefficient $\frac{2\mu^2 + 3\lambda\mu}{\lambda + \mu}$ is called the coefficient of longitudinal elasticity or modulus of elasticity (E)

$$\therefore \quad F = E\,\varepsilon_{\ell} \quad \text{(Hooke's law)}$$

The transversal strain:

$$\frac{\partial v}{\partial r} = \varepsilon_r = \frac{-\lambda}{4\mu^2 + 6\lambda\mu}$$

Where:

v = transversal displacement

ε_r = strain per unit of radial length.

Poisson's ratio (ν) is the ratio between the radial and longitudinal strain

$$\nu = \frac{\frac{\lambda}{4\mu^2 + 6\lambda\mu}}{\frac{\lambda + \mu}{2\mu^2 + 3\lambda\mu}} = \frac{\lambda}{2(\lambda + \mu)}$$

Since E and ν have physical significance and they can readily be determined in elastic materials, they are the constants that appear in most elastic solutions.

Assuming soil an elastic material, attempts have been made to obtain Poisson's ratio from the volumetric changes and vertical displacements that occur in the triaxial test. However Poisson's ratio defined by the simple expression $\frac{\varepsilon_r}{\varepsilon_{\ell}}$ holds only when the cylinder has no lateral constraint. No elastic solution has been attempted for the triaxial test

that permits comparison between the experimental and theoretical volumetric changes and specimen heights. Other problems posed by the triaxial test are that the tangential stress, second intermediate principal stress, is unknown and cannot be controlled; likewise, the effect of the end rigid plate is not known. Quoting Ko and Scott (1968):

> "The stresses and the strain states in the triaxial specimen are both non-uniform and unknown beyond the initial stages of the test, and therefore the stress - strain relationship measured (including failure conditions) is difficult to interpret."

Purpose

It has become quite common to assume soil does not undergo volume changes when it is acted upon by exterior causes; that is, Poisson's ratio is assumed to be 0.5. The fact that theoretical elastic developments are simplified when Poisson's ratio 0.5 is used, together with the abundance of formulas and charts which assume Poisson's ratio 0.5, have created the belief that Poisson's ratio for soils should be taken as 0.5.

This study presents: 1) procedure for the numerical evaluation of Poisson's ratio for a given soil and conditions with an apparatus devised by Dr. R. L. Handy; 2) charts for fast and accurate computations of radial stresses and displacements induced in a semi-infinite elastic medium due to the indentation of a flat ended cylinder; 3) measurement of horizontal radial stresses in soil when the radial displacement

was not controlled; and, 4) an attempt to determine Poisson's ratio for a soil that will be described later.

It is logical to think Poisson's ratio varies for different soils, compactions, moisture contents, temperature, etc; however, the effect of these parameters is beyond the scope of this paper.

Some Theoretical Developments and Experimental Tests on Elastic Half-Space Problems

Taylor (1948) assumes Poisson's ratio zero for the evaluation of the vertical stresses as given by Westergaard's (1938) solution for the elastic half space reinforced by thin strong layers. Peattie (1962) says that for granular and bituminous materials Poisson's ratio is probably between 0.3 and 0.4; Sneddon (1946) using experimental investigation says that Poisson's ratio is approximately 0.25 for dense soils and solid granular materials such as sandstone tested at low pressures.

Since vertical pressure distributions beneath a loaded area are of particular interest for foundation design, numerous experimental investigations have been carried out since the beginning of this century. Results obtained by Koegler and Sheidig (1927), Hugi (1927), Gerber (1929), Aichorn (1931), and Oscar Raber (1933) are presented by Tschbotarioff (1951), where he concluded that the Boussinesq elastic solution could be used with satisfactory accuracy when the soil in question is clay.

In the United States, Spangler and Ustrud (1938), and Foster and Fergus (1951) conducted experimental investigation towards the measurement of stresses induced in a uniform soil by tires and by a flexible circular plate. Experimentation towards the measurement of lateral stresses induced on retaining wall due to surcharge was carried on by Spangler (1938) and by Tschevotarioff and Welch (1948) as cited by Tschevotarioff (1951), and by Mickle (1955).

Since the solution of any three-dimensional problem requires thorough knowledge of elastic theory and utilizes time consuming mathematical techniques, these solutions are less frequent. The first and inspiring determination of stresses and displacements in a semi-infinite, isotropic, elastic medium induced by a point load, was by the French mathematician Boussinesq. Later the mathematician Love (1929) obtained the solution for a flexible, circular plate and a rectangular, flexible footing with uniform applied pressure. Steinbrenner (1936) as cited by Tschevotarioff (1951), published a chart for the computation of vertical stresses beneath the corner of a flexible rectangular footing. Newmark (1942) presented a nomographic solution for the case of a flexible plate that permits computation of stresses induced by flexible footings of any shape. Foster and Alhvin (1954), using Newmark charts, developed new charts that allow faster computation of stresses and displacements beneath a flexible circular plate. Sneddon (1946) computed the distribution of stresses

and displacements caused by the indentation of any rigid solid of revolution, solving specifically for the cases of the sphere, the cone and the flat ended cylinder. Burmister (1945) solved for the distribution of stresses and displacements induced by a flexible plate acting on top of a layered system underlain by a semi-infinite, elastic isotropic medium with no friction between layers. Charyulu (1964) solved the problem for the case when there is friction between the layers and the pressure distributed parabolically on a circular area with the maximum at the center and zero at the edges. Mickle (1955) arrived at a formula that permits computation of induced horizontal stresses in a semi-infinite elastic medium by the application of a uniformly distributed load on a rectangular flexible area.

Suitability of the Elastic Theory

The relatively good comparisons between theoretical developments and experimentation so far indicate that soils may be considered an elastic material within a certain range of pressure; however good comparisons have not been possible, and the following remarks about the matter seem relevant.

For conclusions regarding the suitability of the elastic theory for soils from comparisons, two essential requirements should be met: 1) fulfill experimentally the conditions for which the elastic solution is valid, and 2) obtain measurements free of measuring system errors.

An example of a violation of the first requirement occurred when comparisons were made between the theoretical horizontal stresses induced by surcharge acting on a semi-infinite elastic medium and those stresses measured on a retaining wall (Mickle, 1955). The theoretical solution was obtained by integration of the Boussinesq solution (point load), which implies that each element of load acts independently on the area (Little, 1961); and, for a homogenous, semi-infinite medium, not a semi-infinite medium that contains a yielding wall and a slab foundation made of a material whose elastic properties are different from those of the backfill. The theoretical boundary conditions were not experimentally satisfied.

On the experimental investigation by the corps of engineers (Foster and Fergus, 1951) the surface through which the load was applied introduces some problems. It is generally accepted that tires are flexible, the pressure is uniform and distributed over an area given by the ratio load - inflation pressure; however, due to the stiffness of tires the load is not uniformly distributed and the load - inflation pressure ratio is not a valid criterion for determining the area of contact between a tire and a flexible pavement (Spangler and Ustrud, 1940). Therefore, even tires do not provide the flexibility required to make good comparisons with theoretical developments reached when using the Boussinesq equations.

The second requirement is very difficult if not impossible to fulfill. To claim precision in the measurement of stresses within a soil mass, it is necessary that the measuring device have the same elastic characteristics as the soil; otherwise, a stress concentration will exist. A different case occurs when the stresses to be measured are those exerted by a backfill, or surcharge on a retaining structure; here the measuring device must have the same modulus of elasticity as the material of the retaining structure. This is illustrated by the success of the Carlson cell when used on concrete structures according to Terzhagi and Peck (1968).

This is not to say the previous comparisons were wrong, because they were the best that could be made; however, the departure of the experimental stresses from those that would have been obtained if the theoretical boundary conditions had been satisfied remains unknown.

These considerations suggest that through a better adjustment of the testing boundary conditions to those of the theoretical developments; or through theoretical solutions whose boundary conditions more closely resemble the natural half space soil conditions, it is possible to expect a closer agreement of theoretical and experimental stresses.

Some improvements to the theoretical boundary conditions have been made by Westergaard (1938) who considered an elastic half space reinforced by thin strong layers, and by Wang (1968)

who considered the earth mass a non-linear elastic medium with an elastic modulus varying with the state of stress and with increasing depth due to increasing body forces. A new mechanistic theory, where the time dependence enters into the picture, for computation of stresses and displacements in a soil-water mass has been developed by Ayres, 1966; however, as he states "before the general method can be used to solve real soil mechanics problems much more investigation of physical phenomena must be undertaken.

It is well known that the theory of linear elasticity applies to a material in the range of pressures for which the Hooke's law holds. For metals this proportional limit goes to thousands of p.s.i. for soils it is only a few p.s.i. and varies widely, depending on soil type, compaction, moisture content, and temperature. For computation of stresses through the theory of elasticity it is not required that the material recovers its initial position once the load is released, but that there is stress-strain linearity while the load is being applied. Therefore the use of the elastic theory for soils is reasonable assuming the soil a material whose elastic constants change according to the pressure and that they remain in the range required to elastic materials.

The terms modulus of elasticity and Poisson's ratio will be used throughout this paper. However they are appropriate only for an elastic material which recovers the initial

dimensions once the load is released. The use of Poisson's ratio has the same uncertainties when applied to soils.

Importance of Poisson's Ratio

K. R. Peattie (1962) says that the horizontal stress developed at the bottom of the first layer in a two layer road structure is reduced by from 15% to 22%, with an average decrease of about 19% when Poisson's ratio is changed from 0.5 to 0.35. Other implications of that change are: an increase in vertical stress at the bottom of the second layer by from 2% to 10%, with an average of about 9%; a reduction of the horizontal strain at the base of the first layer from 4% to 17% with an average of about 8%; an increase in the surface deflection from 6% to 9% with an average of about 7%.

Little (1961) using the equation of Borowicka computed a factor (K_r) that determines the contact pressure distribution between a circular slab and the elastic medium on which it rests. With this factor K_r it is possible to enter the proper theoretical curve of contact pressure distribution.

$$K_r = \frac{1}{6} \frac{1 - \nu_S^2}{1 - \nu^2} \frac{E_S}{E} \left(\frac{h}{r}\right)^3$$

Where: ν_S = Poisson's ratio of the slab

ν = Poisson's ratio of the medium

E_S = slab modulus of elasticity

E = medium modulus of elasticity

h = slab thickness

R = slab radius

Tschevotarioff (1951) clearly states that according to the theory of elasticity the at rest pressure in soils is function of Poisson's ratio according to the following relationships:

$$\varepsilon_3 = \frac{1}{E} [\sigma_3 - \nu(\sigma_1 + \sigma_2)]$$

Where: E = elastic modulus of the soil

ε_3 = lateral strain

σ_2 and σ_3 = lateral stresses

σ_1 = vertical stress

ν = Poisson's ratio of the soil

In a soil mass with a level free surface $\sigma_2 = \sigma_3$. In the at rest pressure condition, by definition, there is no lateral deformation

($\varepsilon_3 = 0$) $$0 = \frac{1}{E} [\sigma_3 - \nu(\sigma_1 + \sigma_3)]$$

$$\sigma_3(1 - \nu) = \nu\sigma_1$$

By definition the at rest pressure ratio (K_n) is:

$$K_n = \frac{\sigma_3}{\sigma_1}$$

$$\therefore \quad K_n = \frac{\nu}{1 - \nu}$$

Thus, it appears that the determination of an elastic constant similar to Poisson's ratio has practical value for the adequate theoretical solution of some soil engineering problems.

CHAPTER II: IDEALIZED OPERATION OF A PRESSURE MEASURING DEVICE

A Pressure Measuring Device

The device used in the experimentation is the one illustrated in Figure 1.

The device consists of the following parts as shown in Figure 1.

1 Hydraulic Manual Pump.

2 Pressure Gauge.

3 Cylinder, within which a piston can move according to the pressure direction.

4 Metallic plate at the end of the piston rod on which the lateral pressures are exerted.

5 Calibrated strain gauge attached to the piston rod that measures piston displacements.

6 Strain indicator.

The device thus consists of an hydraulic system that allows the measurement of pressures exerted on the contact plate; and, of an electric strain gauge which permits the recording of displacements in terms of strain readings.

The unit pressure exerted on the contact plate is obtained through the simple relationship:

$$P_p \times A_p = P_P \times A_P$$

$$P_p = \frac{P_P \times A_P}{A_p}$$

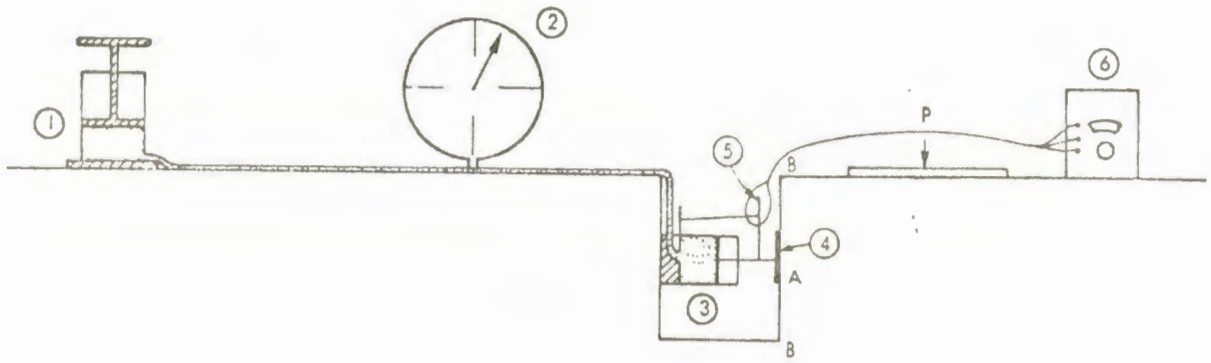

Figure 1. The pressure measuring device

Where:

P_p = unit pressure on contact plate

A_p = contact plate area

p_p = unit pressure on piston. (Pressure gauge reading)

A_p = piston area.

Since the area of the piston used in the device is 1 in^2

$$P_p = \frac{\text{Pressure Gauge Reading}}{\text{Contact Plate Area}}$$

The device has a contact plate area of 5.0 in^2.

A unique feature of this device is that the piston displacement can be controlled by exerting, through the hydraulic pump, the pressure required to maintain an arbitrary strain reading. The device also makes it possible to apply an arbitrary contact pressure.

The pressure gauge used is temperature compensated for a range of 0°F to 100°F, so that pressures readings are not affected by temperature in this range.

Its use in an idealized operation

Consider a perfectly elastic, homogenous isotropic medium, in which a hole has been bored in order to place the device at different depths within the medium. With the hydraulic pump a contact pressure p_o is applied so that point A (see Figure 1) has the same system of forces in equilibrium it had before the hole was bored.

If the hole is filled with the same elastic medium, the system of forces in equilibrium on plane B-B is the same as before the hole was bored. When a given unit pressure P is applied on the bearing plate, a certain horizontal stress is induced at point A that, with little error because of the small plate area, may be computed as the total horizontal stress on the plate divided by its area.

Spring Analogy

The hydraulic system in the bore-hole and the soil around it may be thought of as two springs of different modulii of elasticity, each with an end at point A as shown in Figure 2.

The modulus of elasticity of the hydraulic system is E_s, and that of the elastic medium is E_m. The following three steps outline the measuring procedure.

1. The contact pressure is applied, so that the forces in equilibrium in point A simulate the forces at that point before the hole was bored. Call the pressure gauge reading p_o and the strain indicator reading s_o.

2. The applied vertical load creates a horizontal stress P_1, displacing point A a distance S_1, and causing a total displacement Δt_1 at B. The displacement at B must be the addition of the strains in the system (ΔS_1) and in the soil (ΔM_1).

$$\Delta t_1 = \Delta S_1 + \Delta M_1 .$$

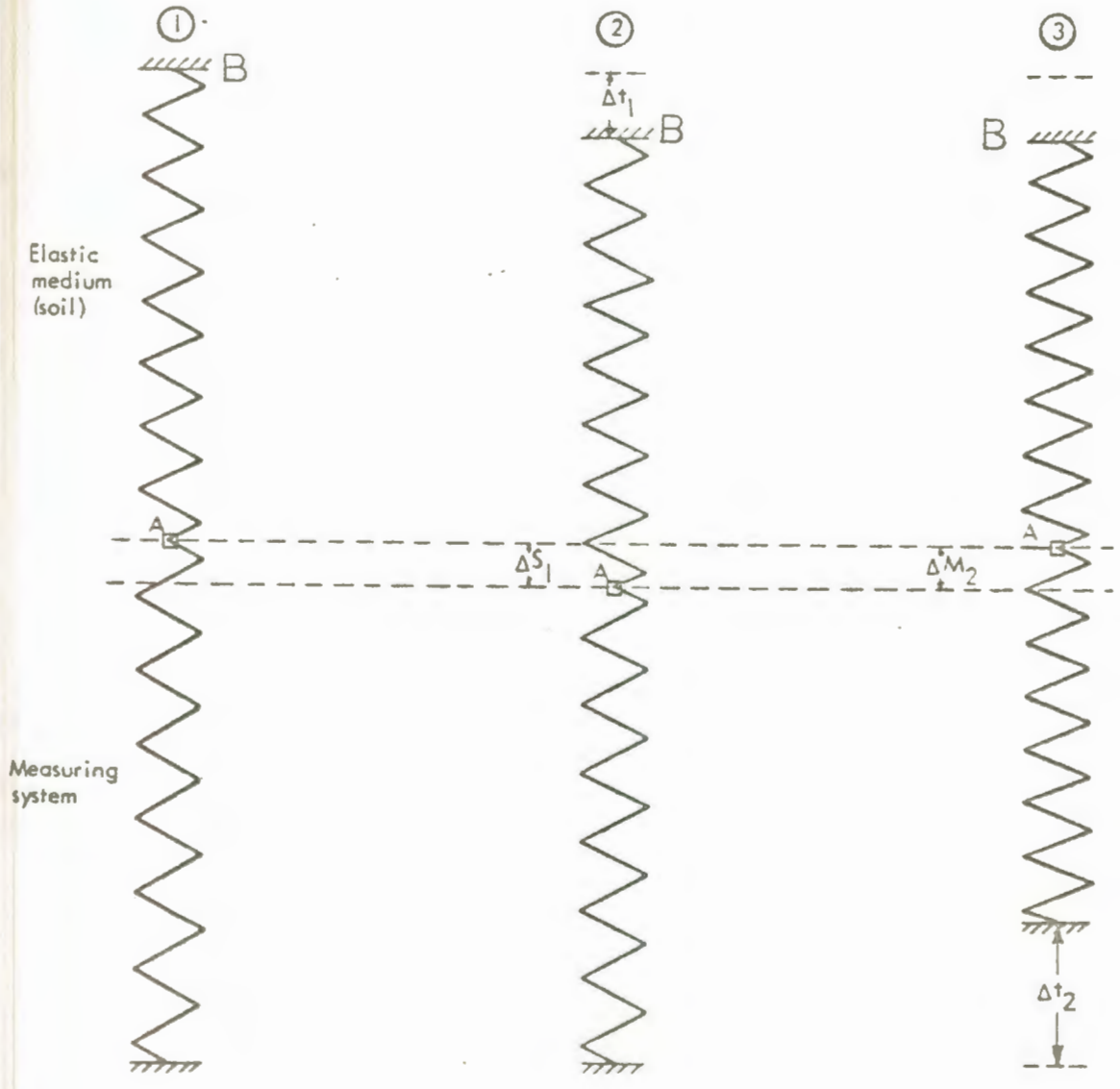

Figure 2. Spring analogy

Call the new pressure gauge reading p_1 and the new strain indicator reading s_1.

$$\Delta S_1 = S_1 - S_o$$

$$P_1 = p_1 - p_o$$

3. A force P_2 is applied to overcome the displacement of point A. The total displacement Δt_2 must be the addition of the strains in the measuring system ΔS_2 and in the soil ΔM_2. Call the new pressure gauge reading P_2. The strain indicator reading must be:

$$\Delta M_2 = S_o - S_1 = -(S_1 - S_o)$$

$$P_2 = p_2 - p_1$$

As can be seen the displacement measured by the strain indicator in step 2 of the sequence is that of the measuring system, and in step 3 is that of the soil; therefore, the following relationship can be written:

$$\Delta S_1 = M_2 \quad (1)$$

According to Hooke, the force is proportional to the stretch

$$P = E \times \Delta S$$

Where:

P = force

E = spring modulus

ΔS = spring stretch or shortening.

Expression (1) can be written:

$$\frac{P_1}{E_S} = \frac{P_2}{E_M}$$

$$\therefore \quad P_1 = \frac{E_S}{E_M} P_2 \quad (2)$$

If a stress - displacement (or strain reading) is plotted, it may look like the one shown in Figure 3.

To test the device's behavior a lab simulation was devised as shown in Figure 4 and an experimental curve that conforms to the analytical equation (2) was found. Figure 5 is one example; the first point of the third step is somewhat displaced probably due to piston twisting.

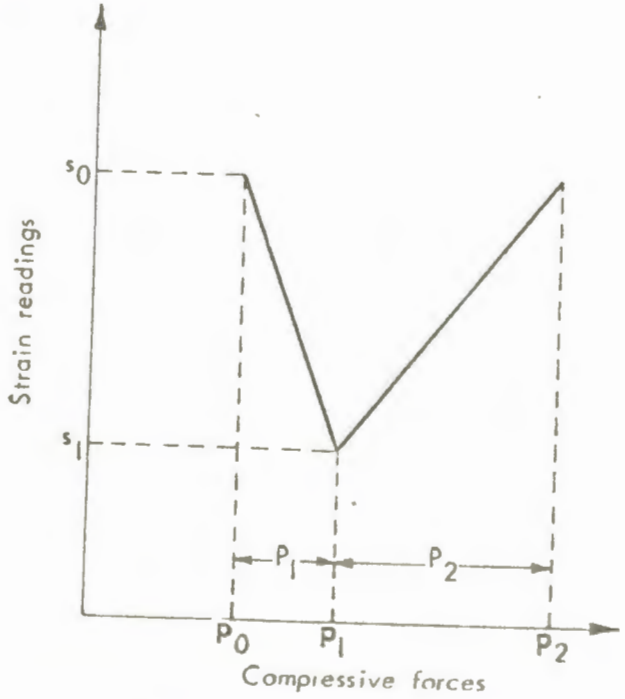

Figure 3. Theoretical stress-strain relationship

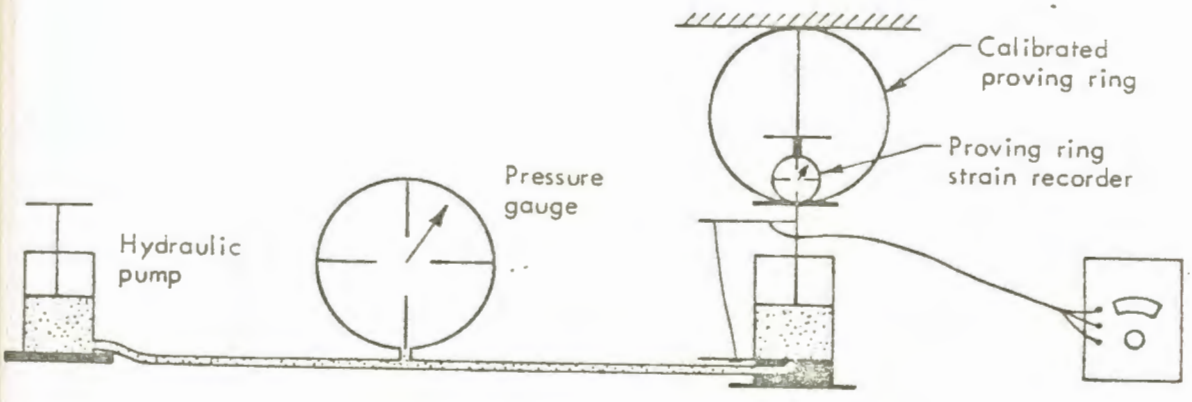

Figure 4. Lab simil

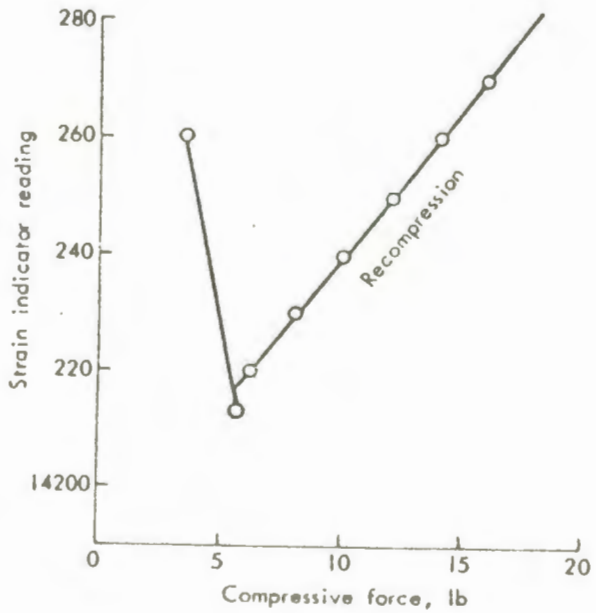

Figure 5. Lab simil stress-strain relationship

CHAPTER III: MEASUREMENTS IN SOIL WHEN THE RADIAL DISPLACEMENT WAS NOT CONTROLLED

Soil Description

The soil used for field tests is the glacial till described by the engineering properties in Table 1.

Table 1. Soil analysis

Size fraction	Size in milimeters	Percent by weight
Gravel	larger than 2.0	4.3%
Coarse sand	2.0 to 0.42	11.8%
Fine sand	0.42 to 0.05	53.3%
Silt	0.05 to 0.005	19.7%
Clay	smaller than 0.005	10.9%

Effective size, in millimeters	0.0042
Uniformity coefficient	33.4

Atterberg limits

Liquid limit	35.3
Plastic limit	17.7
Plasticity index	17.6

Average densities the day the plate bearing test was run:

Dry density	116.1 p.c.f.
Wet density	129.0 p.c.f.

The atterberg limits tests classify this soil as a silty clay of low to medium plasticity and low to medium compressibility according to the Casagrande Soil Classification, or as an A-6 soil according to the Highway Research Board Classification.

Measurements in Soil

The device was inserted in 6-in. diameter holes, and the load was applied via a 12-in. diameter plate with load test truck.

The recorded stresses are not equal to those that would build up naturally at the tested depths and offset distances if no hole had been bored. This is due to the difference between modulus of elasticity of the measuring system and that of the soil, the impossibility of simulating the system of forces in equilibrium in the walls of the hole before it was bored. Other factors affecting the reliability of the measurements are: the area of the contact plate of the device giving an average pressure and the daily variation in soil properties, especially moisture content.

The effect of consolidation upon pressure readings can be seen in Figure 6 where points III, III', III" and III"' correspond to the same hydraulic pressure pump movement and should result in the same pressure.

Observations

Transmitted horizontal pressures are shown for the following cases:

1. Measurements at the bottom of the open bore-hole, in which the device is allowed to compress.

2. Measurements taken as in number 1 but with a cylinder of sheet metal against the walls of the hole above the device

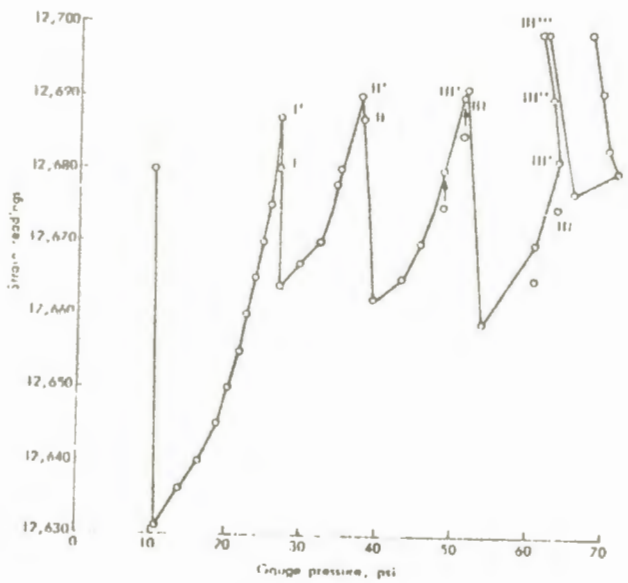

Figure 6. Effect of consolidation on pressure readings

to comprise a more or less rigid inclusion.

3. Measurements taken as in No. 1 but with no displacement allowed at the interface of the device and the soil.

All graphs of measured horizontal stresses vs. applied vertical pressure show linearity. For comparison theoretical lateral pressures computed from Boussinesq Theory are shown. Figures 7 and 8 result from the conditions of case 1.

Comparison of Figures 7(A) and (B) demonstrates that the induced lateral stresses at 2-ft. depth decrease with increasing load-offset distance.

A comparison of Figures 8(A) and (B) show that the induced lateral stresses decrease with depth for the same offset distance.

The initial contact pressure has an effect upon the measured stresses, greater stresses occurring with lower initial contact pressures, as shown in Figure 8(A).

If the device is recompressed upon application of vertical load so that no displacement is allowed at the interface of measuring system-soil, Case 3, the measured stresses are higher, as indicated by comparing lines II and III in Figure 9.

Measurements with the semi-rigid inclusion, Case 2, were not linear, suggesting that the rigidity of the inclusion changed with pressure. This graph is not presented, and this particular technique was abandoned.

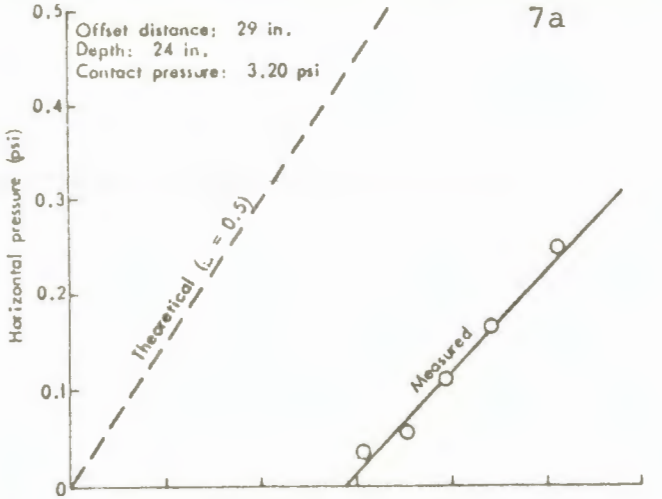

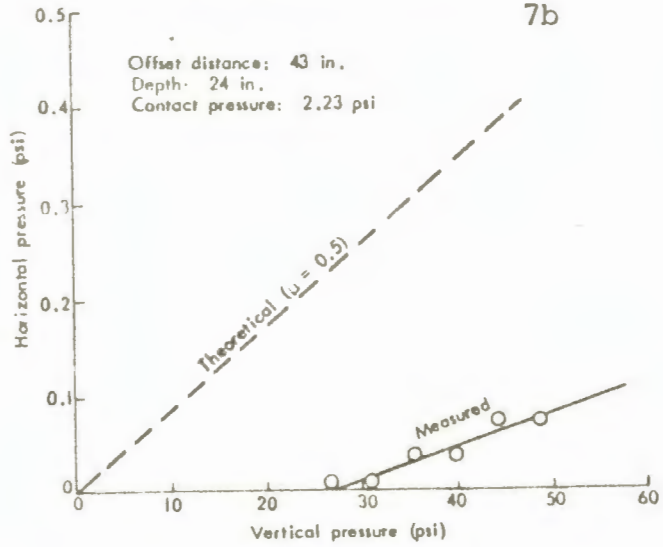

Figure 7. Experimental stresses-radial displacement not controlled

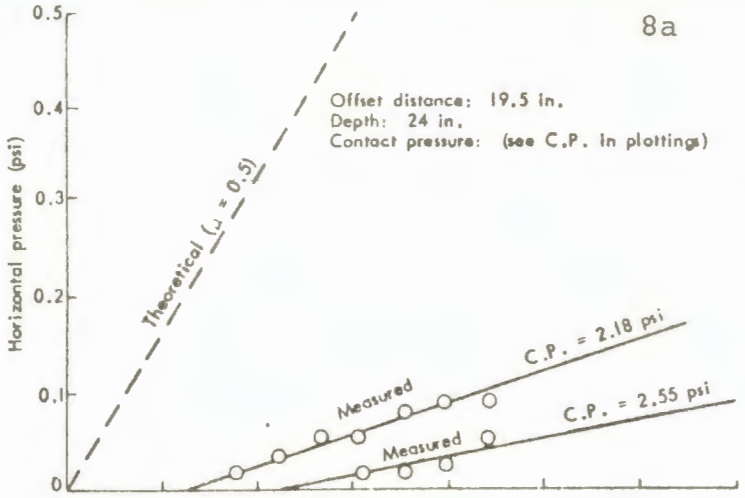

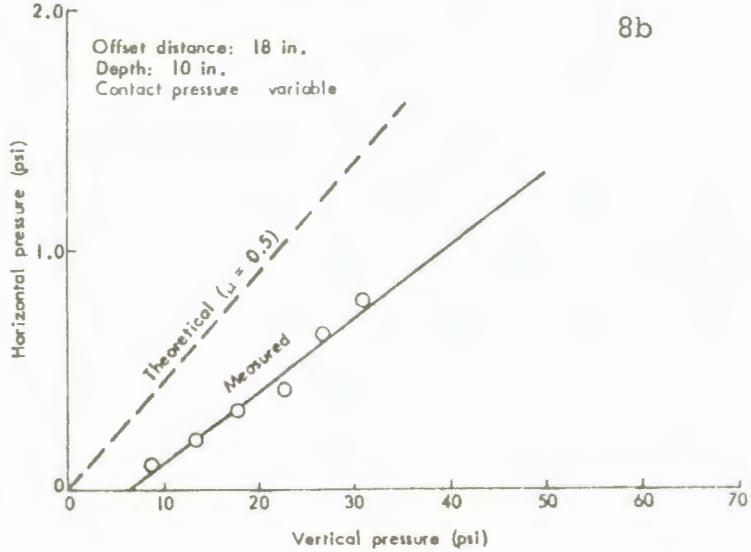

Figure 8. Experimental stresses-radial displacement not controlled

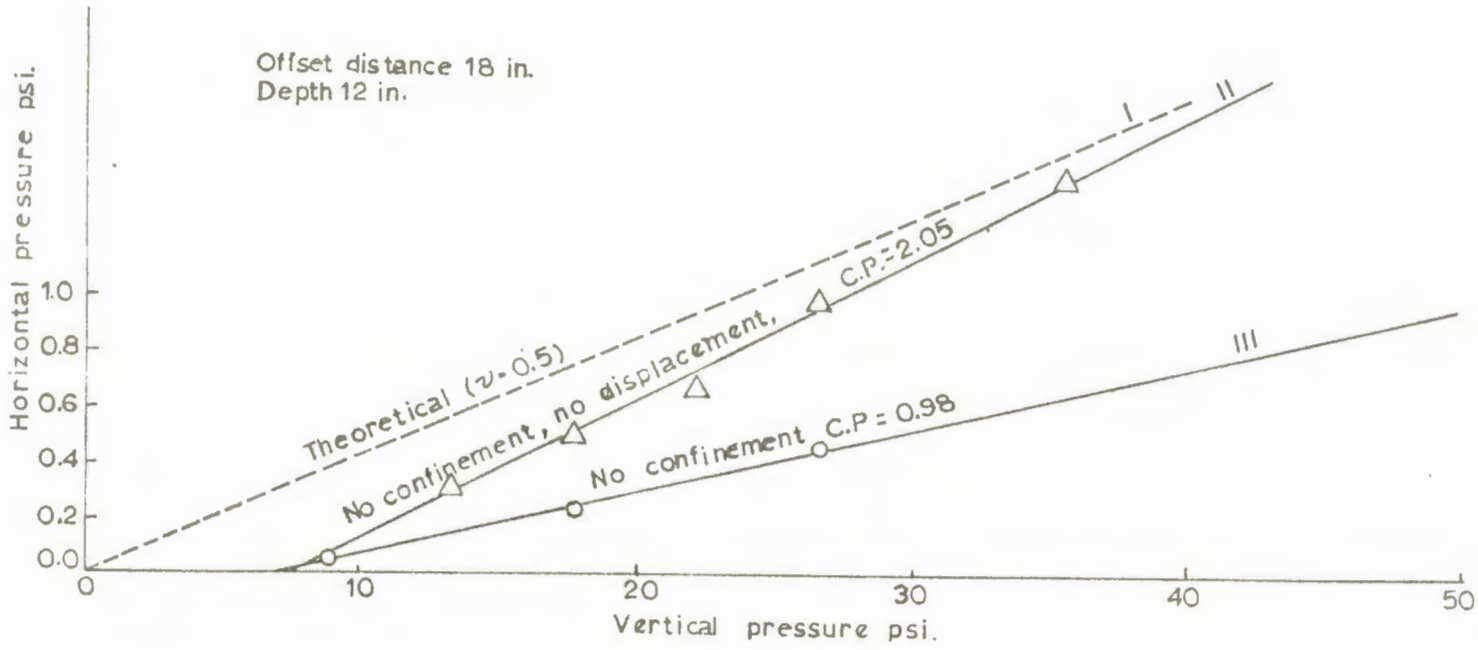

Figure 9. Recorded experimental stresses when no radial displacement was allowed

In all graphs measured values of lateral pressures vs. vertical pressures have intercepts on the vertical pressure axis; in other words, indicating a minimum vertical pressure below which no lateral compressive stresses could be measured with the equipment for a given depth, offset distance and contact pressure.

Discussion

From the linearity between the vertical and horizontal pressures, it is possible to say that for a given depth and offset distance, the lateral pressure is a function of Poisson's ratio as is expected; however nothing can be said yet about its value and about the constancy or variability of this ratio for different depths. The displacement has not been controlled and the theoretical lateral stresses are based upon the assumption of a load applied via a flexible plate and not for the rigid bearing plate used in the experiment.

The intersection of the straight lines formed by the measured values with that of zero for lateral pressure correspond to a certain vertical pressure greater than zero. This suggests that at a given depth and offset distance, below this minimum vertical pressure the horizontal stresses are tensile stresses. It may be that if the at rest pressure is used rather than the arbitrary contact pressures, the intercept will move to zero vertical pressure.

Assuming that curves I and II of Figure 9 both had the same origin at zero, all the measured lateral stresses would be greater than the theoretical. This is expected since curve II was obtained when no displacement was allowed. It is well known that the lateral stresses acting on retaining walls varies inversely to the outward movement.

The spring analogy furnishes an analytical proof of the necessity for the linear stress-strain curves for both the loading and the recompression phase of the test. The spring analogy holds perfectly in the lab test; however, the lab test is far from being a good replica of the field conditions mainly because the proving ring has linear stress-strain behavior and the soil does not. Also the stress condition above the device that exists in the field is not present in the lab simil, and the displacement allowed by the measuring system modulus of elasticity is different from that of the soil. In order to get a true measurement it will be necessary for the device to simulate the stress-strain characteristics of the soil.

Although the measurements made in the experiment are not true values of lateral stresses, they do indicate the possibility of using this measuring concept. It is most important that the displacement be controlled. These preliminary tests suggest a revised procedure whose target is the numerical solution of Poisson's ratio for a given soil, and the establishment of criteria for computation of induced horizontal stresses.

CHAPTER IV: DESCRIPTION OF THE EXPERIMENTAL METHOD FOR POISSON'S RATIO DETERMINATION

Description of the Method

From the spring analogy it can be concluded that three cases of lateral stress conditions are possible:

1. When Es > Em, P1 > P2
2. " Es = Em, P1 = P2
3. " Es < Em, P1 < P2

In case #1 the measuring device acts as a rigid inclusion, and in case #3, as a soft inclusion. The only case when the recorded stresses P1 correspond to those that would naturally develop in the elastic medium is in case #2 where the elastic modulii of the soil and measuring system are equal.

The device can be used in a manner which controls displacement, therefore the following procedure for Poisson's ratio determination is proposed:

1. Find a theoretical relationship between stresses and displacements from elastic theory for a particular case. The one used here is "Boussinesq problem for a flat ended cylinder". The theoretical solution for stresses and displacements within a semi-infinite elastic mass was obtained through singular mathematical achievement by Sneddon (1946) and is used here because with the available testing facilities it is possible to establish good agreement with the theoretical boundary conditions. Also the solution is complete for stresses and

displacements, and through simple algebraic manipulations of the equations, it is possible to arrange them so that a computer program can be written for the numerical evaluation of the factors that affect stresses and displacements. With the computer results it was possible to draw, graphs that permit fast and accurate computations of stresses and displacements for any plate diameter, pressure, medium, modulus of elasticity and Poisson's ratios of .25, .30, .35, .40, .45, .50. The computer program is presented in the Appendix.

2. Obtain the soil modulii of elasticity that correspond to different pressures from the results of a plate bearing test and the following analysis. According to Harding and Sneddon (1946) the resultant pressure is given by the expression:

$$P = \frac{2}{1 - \nu^2} E \, \Delta a$$

The stress delivered by the rigid plate is:

$$P = p(\pi a^2)$$

Replacing in Sneddon's expression, and solving for the modulus of elasticity (E) we obtain:

$$E = \frac{1.5708(1 - \nu^2)}{\Delta} \, pa$$

Where:

E = modulus of elasticity

ν = Poisson's ratio

p = plate unit pressure

a = plate radius

Δ = vertical displacement.

When this expression is evaluated for Poisson's ratio of 0.5, it becomes the well known identity $E = 1.18 \frac{pa}{E}$ presented by Yoder (1959).

3. Fulfill experimentally the boundary conditions for which the elastic theoretical solution is valid. This requirement was accomplished by using a rigid circular plate for the surface load. It is obvious that the elasticity requirement for the semi-infinite medium can not be fulfilled; however, the procedure to be used avoids this requirement by using the soil modulus of elasticity that corresponds to each particular load and the assumption that for a particular pressure the soil modulus of elasticity has to be the same at the surface and within the mass.

4. Compute from the theoretical solution radial displacements and stresses that correspond to different vertical pressures and Poisson's ratios, for different points within the mass.

5. Place the measuring device at different depths and offset distances, applying a contact pressure equal to the calculated at rest pressure for that depth which will be one half the depth times the unit weight of the soil.

6. Restore the system of forces in equilibrium that existed above the device before the hole was bored. Strictly,

the only way of restoring the condition that existed prior to boring the hole is to refill the hole with the same material at the same density.

7. A given vertical stress is applied at the surface of the soil and the pressure gauge readings increase according to the displacement allowed by the device. Once the computed theoretical displacement, for a fixed Poisson's ratio, is reached, it will be held constant by pumping the hydraulic pump, and the pressure reading taken at the moment the needle of the strain indicator shows that consolidation of the soil is starting. If a stress-displacement graph is plotted, it should look like the one shown in Figure 10 provided the elastic modulus of the measuring system is less than that of the soil.

8. Hold the vertical pressure constant and repeat step #7 for displacements that correspond to different Poisson's ratios.

9. Repeat the procedures of steps 7 and 8 for greater vertical pressures and plot experimental radial stresses versus vertical pressure for different Poisson's ratios, and on the same graph plot the theoretical radial stresses versus vertical pressures as is shown on the hypothetical Figure 11.

10. For a given vertical pressure the correct value of Poisson's ratio will be the one for which the theoretical and the experimental radial stresses are identical. The dotted line in Figure 11 indicates a case in which Poisson's ratio

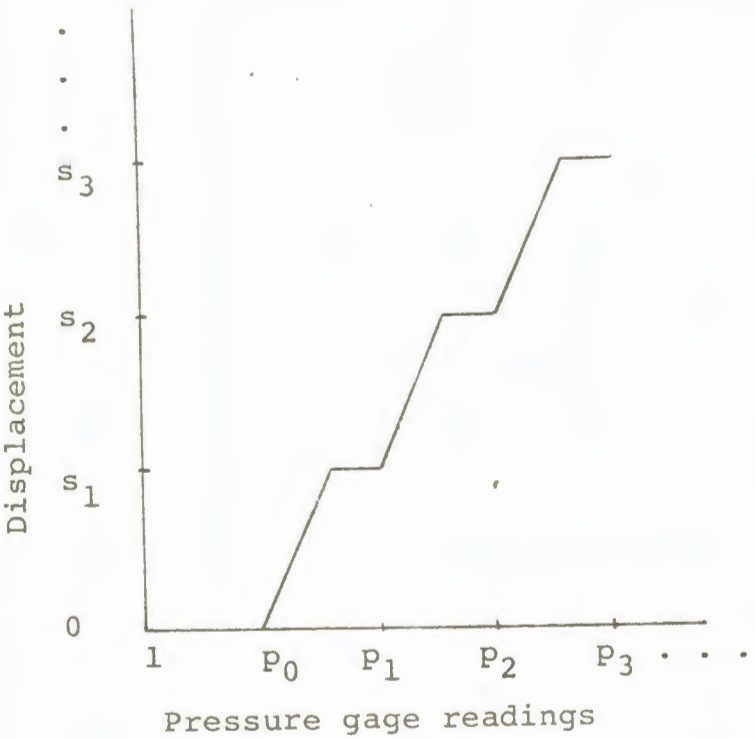

p_0 at rest pressure (contact pressure)

$p_1 - p_0$, $p_2 - p_0$,..., $p_n - p_0$ are recorded horizontal stresses correspondent to the theoretical horizontal displacements: $s_1 - s_0$, $s_2 - s_0$,..., $s_n - s_0$

Figure 10. Illustration of step 7

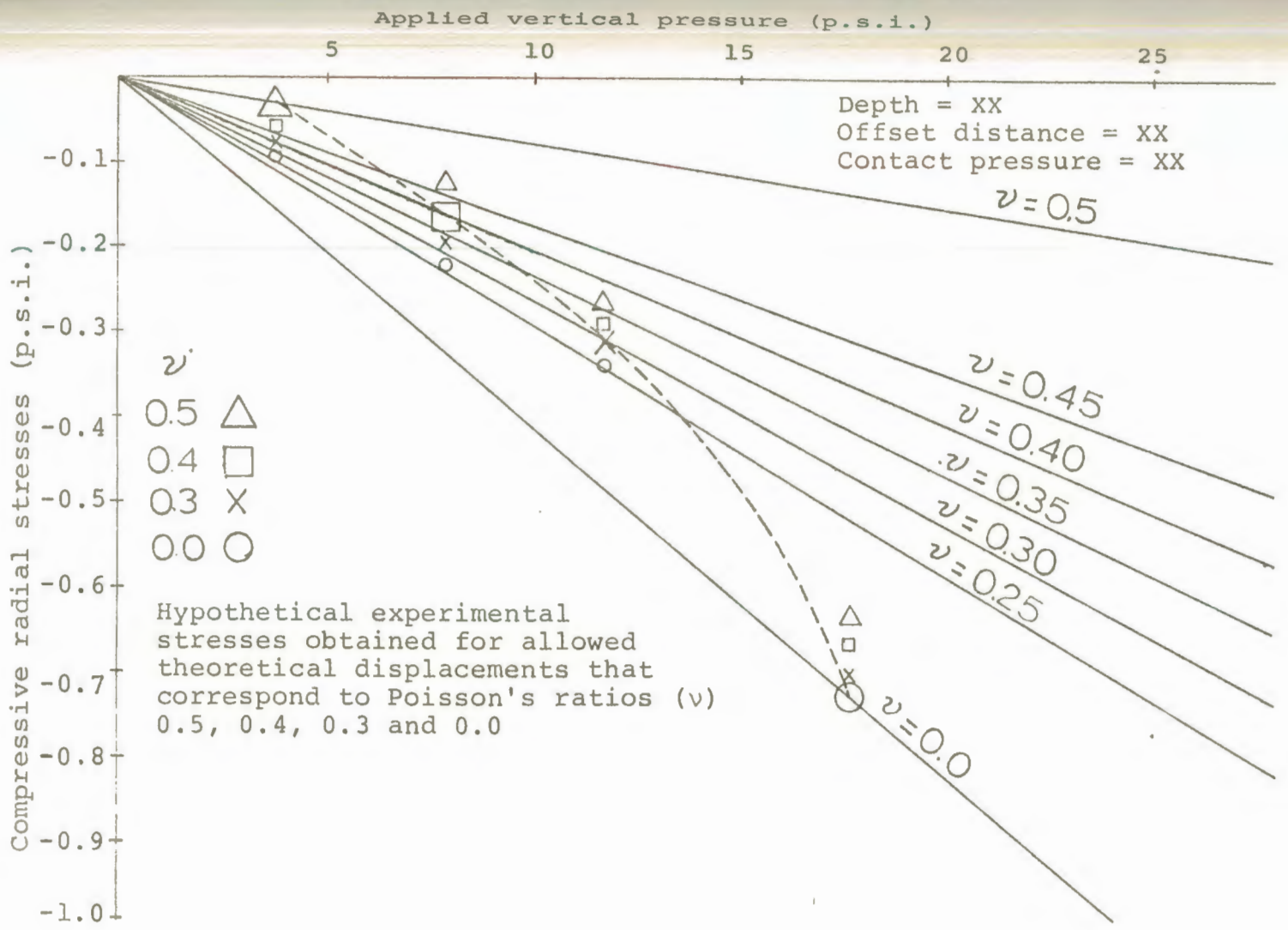

Figure 11. Illustration of steps 9 and 10

decreases for increasing vertical pressure. Lengthy theoretical computations, careful handling of the equipment and the solution of practical problems are required; however, the method offers an in situ, experimental approach to the computation of Poisson's ratio in soils.

Discussion of the Method

The initial contact pressure used is one half depth times the unit weight of the soil that is approximately the at rest pressure. Little error is introduced because as will be seen later Poisson's ratio for the at rest condition at small depths probably is between 0.5 and 0.3. The arbitrary chosen contact pressure correspond to Poisson's ratio 0.33 according to the following analysis:

$$\text{Used at rest pressure} = K_m = 0.5 = \frac{\nu}{1 - \nu}$$

$$\therefore \quad \nu = 0.33$$

With the actual device it is not practical to fill the hole once the device is inserted; therefore the requirement #6 has not been fulfilled. An ideal test is possible at 1" depth because the soil provides confinement at lower depths and the plate covers the remaining part of the soil. The effect of the hole remains unknown.

The size of the contact plate limits the accuracy of the experimental recorded stresses since it produces an average

plate stress, which is compared to a theoretical stress that corresponds to the plate center point. The plate area is small and it probably is not a source of major error. An estimate of the introduced error can be furnished when results from smaller size plates are available.

All these sources of errors can be minimized through experimentation; however due to time limitations these corrective measures have not been made.

CHAPTER V: TRANSFORMATION OF SNEDDON'S SOLUTION EQUATIONS FOR THE BOUSSINESQ PROBLEM FOR THE CASE OF A FLAT ENDED CYLINDER

The Transformation

According to Sneddon (1946) elastic mathematical analysis, the stresses and displacements caused by the indentation of a flat ended cylinder in an elastic isotropic half space (see Figure 12) are given by the expressions:

$$\sigma_z = -\frac{4\mu(\lambda + \mu)}{\lambda + 2\mu} \frac{\Delta}{\pi a} (J_1^0 + \zeta J_2^0)$$

$$T_{zr} = -\frac{4\mu(\lambda + \mu)}{\lambda + 2\mu} \frac{\Delta}{\pi a} \zeta J_2^1$$

$$\sigma_\theta = -\frac{4\lambda\mu}{\lambda + 2\mu} \frac{\Delta}{\pi a} J_0^1 - \frac{4\mu}{\rho(\lambda + 2\mu)} \frac{\Delta}{\pi a} (J_0^1 - \frac{\lambda + \mu}{\mu} \zeta J_2^1)$$

$$\sigma_r + \sigma_\theta = -\frac{4\mu}{\lambda + 2\mu} \frac{\Delta}{\pi a} (2\lambda + \mu) J_1^0 - (\lambda + \mu)\zeta J_2^0$$

$$u_r = -\frac{2\mu}{\lambda + 2\mu} \frac{\Delta}{\pi} (J_0^1 - \frac{\lambda + \mu}{\lambda} \zeta J_1^1)$$

$$u_z = \frac{2\Delta}{\pi} (J_0^0 + \frac{\lambda + \mu}{\lambda + 2\mu} \zeta J_1^0)$$

Where:

σ_z = vertical stress

$T_{r\theta}$, $T_{z\theta}$, T_{zr} = shearing stresses

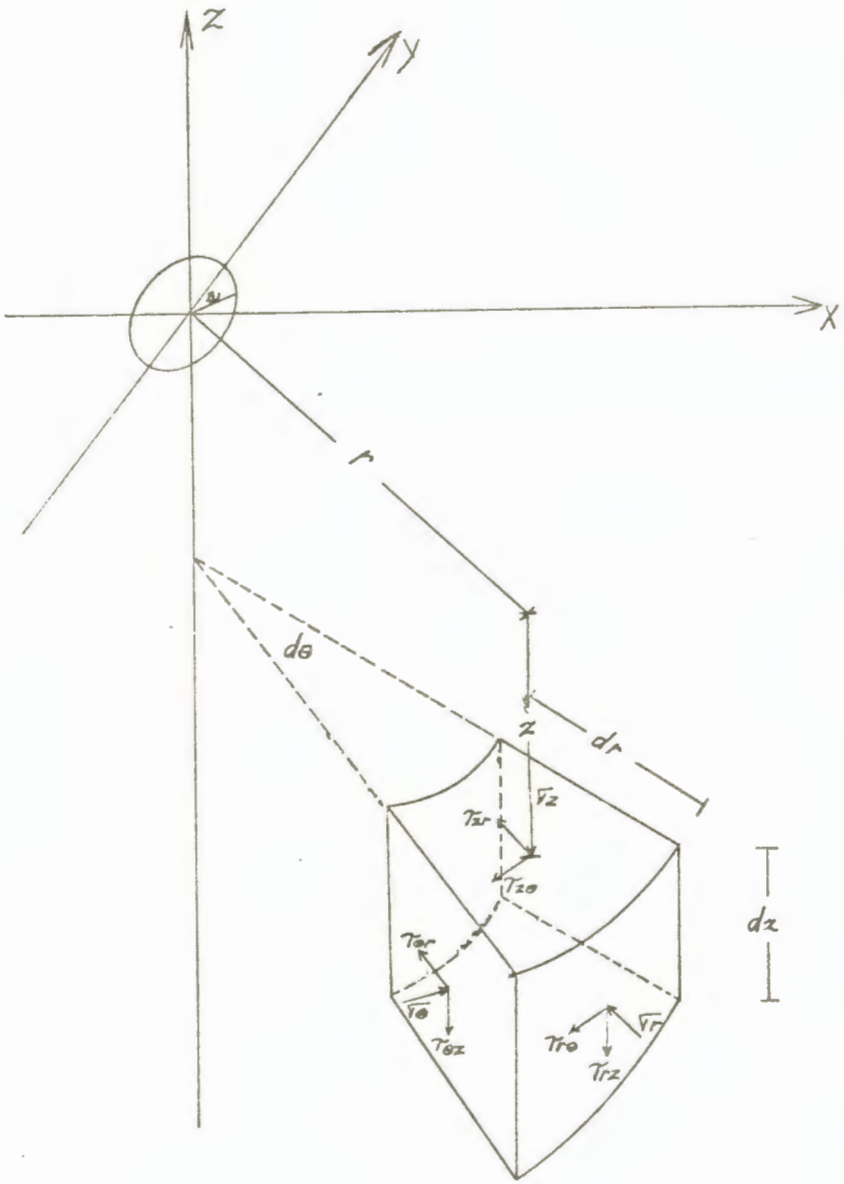

Figure 12. Stresses acting on an infinitesimal element located at depth z and offset distance r from the center of the plate

σ_θ = tangential stress

σ_r = radial stress

u_r = radial displacement

u_z = vertical displacement

λ, μ = Lame's elastic constants of the deformed medium

Δ = distance the cylinder penetrates below the level of the undisturbed boundary

$\rho = \frac{r}{a}$

$\zeta = \frac{z}{a}$

r = horizontal distance from the center of the flat ended cylinder to the point in consideration

z = vertical distance from surface to the point in consideration

a = plate radius.

$$J_n^m = \int_0^\infty p^{n-1} \sin p e^{-p\zeta} J_m(p\zeta)\, dp = \text{imaginary part of}$$

$$\int_0^\infty p^{n-1} e^{-p(\zeta-i)} J_m(p\zeta)\, dp$$

Sneddon solved the Bessel functions involved in the solution and obtained:

$$J_1^0 = R^{-1/2} \sin\tfrac{1}{2}\phi \qquad J_2^0 = rR^{-3/2} \sin\tfrac{3}{2}(\phi - \theta)$$

$$J_0^1 = \frac{1}{\rho}(1 - R^{1/2} \sin\tfrac{1}{2}\phi) \qquad J_1^1 = r\zeta^{-1} R^{-1/2} \sin(\theta - \tfrac{1}{2}\phi)$$

$$J_2^1 = \rho R^{-3/2} \sin\tfrac{3}{2}\phi$$

Where:

$$r^2 = 1 + \zeta^2 \qquad \tan \theta = \frac{1}{\zeta}$$

$$R^2 = (\rho^2 + \zeta^2 - 1)^2 + 4\zeta^2 \qquad \tan \phi = \frac{2\zeta}{\rho^2 + \zeta^2 - 1}$$

In order to obtain expressions as function of pressure, modulus of elasticity and Poisson's ratio, use was made of the following equations:

$$\Delta = \frac{\pi}{2} (1 - \sigma^2) \frac{pa}{E} \qquad (a)$$

$$\mu = \frac{E}{2(1 + \sigma)} \qquad (b)$$

$$\lambda = \frac{E\sigma}{(1 + \sigma)(1 - 2\sigma)} \qquad (c)$$

(a) was obtained by equating the total applied pressure $P = p\pi a^2$ to the Sneddon expression for the resultant pressure on the pressed area: $P = \frac{2}{1 - \sigma^2} E\Delta a$ and solving for Δ.

(b) and (c) are equalities furnished by the theory of elasticity.

The meaning of the symbols in these expressions is:

p = unit applied pressure

μ, λ = Lame's elastic constants

E = modulus of elasticity

σ = Poisson's ratio

a = plate radius.

After performing these substitutions and the corresponding algebraic simplifications (see Appendix), the following expressions are obtained:

$$\sigma_z = - \frac{p}{2} (J_1^0 + \zeta J_2^0)$$

$$T_{zr} = - \frac{p}{2} \zeta J_2^1$$

$$\sigma_\theta = - p\sigma J_0^1 - \frac{p}{2\rho} (1 - 2\sigma)(J_0^1 - \frac{\zeta}{1 - 2\sigma} J_2^1)$$

$$\sigma_r + \sigma_\theta = - \frac{p}{2} ((2\sigma + 1)J_1^0 - \zeta J_2^0)$$

$$u_r = - \frac{(1 - 2\sigma)(1 + \sigma)}{2} \frac{pa}{E} (J_0^1 - \frac{1}{2\sigma} \zeta J_1^1)$$

$$u_z = (1 - \sigma^2) \frac{pa}{E} (J_0^0 + \frac{1}{2(1 - \sigma)} \zeta J_1^0)$$

From the expressions it can be seen that the vertical stresses and the shearing stresses are independent of the medium elastic constants; however, the tangential and radial stresses as well as the radial and vertical displacements depend on the medium modulus of elasticity and Poisson's ratio.

In order to visualize quantitatively the distribution of stresses, it is convenient to express the stresses as a percentage of the applied unit pressure; and, in order that a

general practical use of the expressions for the displacements be made, it is convenient to determine a factor that when multiplied by the unit pressure and cylinder radius and when divided by the medium modulus of elasticity yields the corresponding displacement. Once the corresponding manipulations are performed, the following expressions are obtained:

$$(1)\quad 100\,\frac{\sigma_z}{p} = -\,50(J_1^0 + \zeta J_2^0)$$

$$(2)\quad 100\,\frac{T_{zr}}{p} = -\,50\,\zeta J_2^1$$

$$(3)\quad 100\,\frac{\sigma_\theta}{p} = -\,100\,\nu J_0^1 - \frac{50(1-2\nu)}{\rho}\left(J_0^1 - \frac{\zeta}{1-2\nu}\,J_2^1\right)$$

$$(3')\quad 100\,\frac{\sigma_r + \sigma_\theta}{p} = -\,50[(2\nu+1)J_1^0 - \zeta J_2^0]$$

$$(4)\quad 100\,\frac{\sigma_r}{p} = -50[(2\nu+1)J_1^0 - \zeta J_2^0] + 100\,\nu J_0^1 + \frac{50(1-2\nu)}{\rho}\left(J_0^1 - \frac{\zeta}{1-2\nu}\,J_2^1\right)$$

$$(5)\quad u_r\left(\frac{E}{pa}\right) = -\,\frac{(1-2\nu)(1+\nu)}{2}\left(J_0^1 - \frac{1}{2\nu}\,\zeta J_1^1\right) = F_r$$

$$(6)\quad u_z\left(\frac{E}{pa}\right) = (1-\nu^2)\left(J_0^0 + \frac{1}{2(1-\nu)}\,\zeta J_1^0\right) = F_\nu$$

The expressions (1), (2), (3), (4) and (5) were computer programmed by Mr. Russell Fish and Mr. Kenneth Bergeson. Expression (6) was not evaluated because the solution of the Bessel function J_0^0 is not presented by Sneddon.

In expressions (1) through (6) ν has replaced σ since ν is actually a more popular symbol for Poisson's ratio.

In the Appendix computations are also for a given depth, offset distance, modulus of elasticity and Poisson's ratio. The purpose of this set of computations was to check the reliability of the computer program and the transformation made to Sneddon's equations into the expressions (1), (2), (3), (4), and (5) furnished above. The perfect agreement between the computer values and those obtained by hand proves that the transformations and the computer program are correct.

Charts for Computation of Horizontal Radial Stresses and Displacements

The charts that follow were obtained by plotting the numerical data, furnished by the computer, that correspond to radial stresses and displacements versus depth for fixed offset distances.

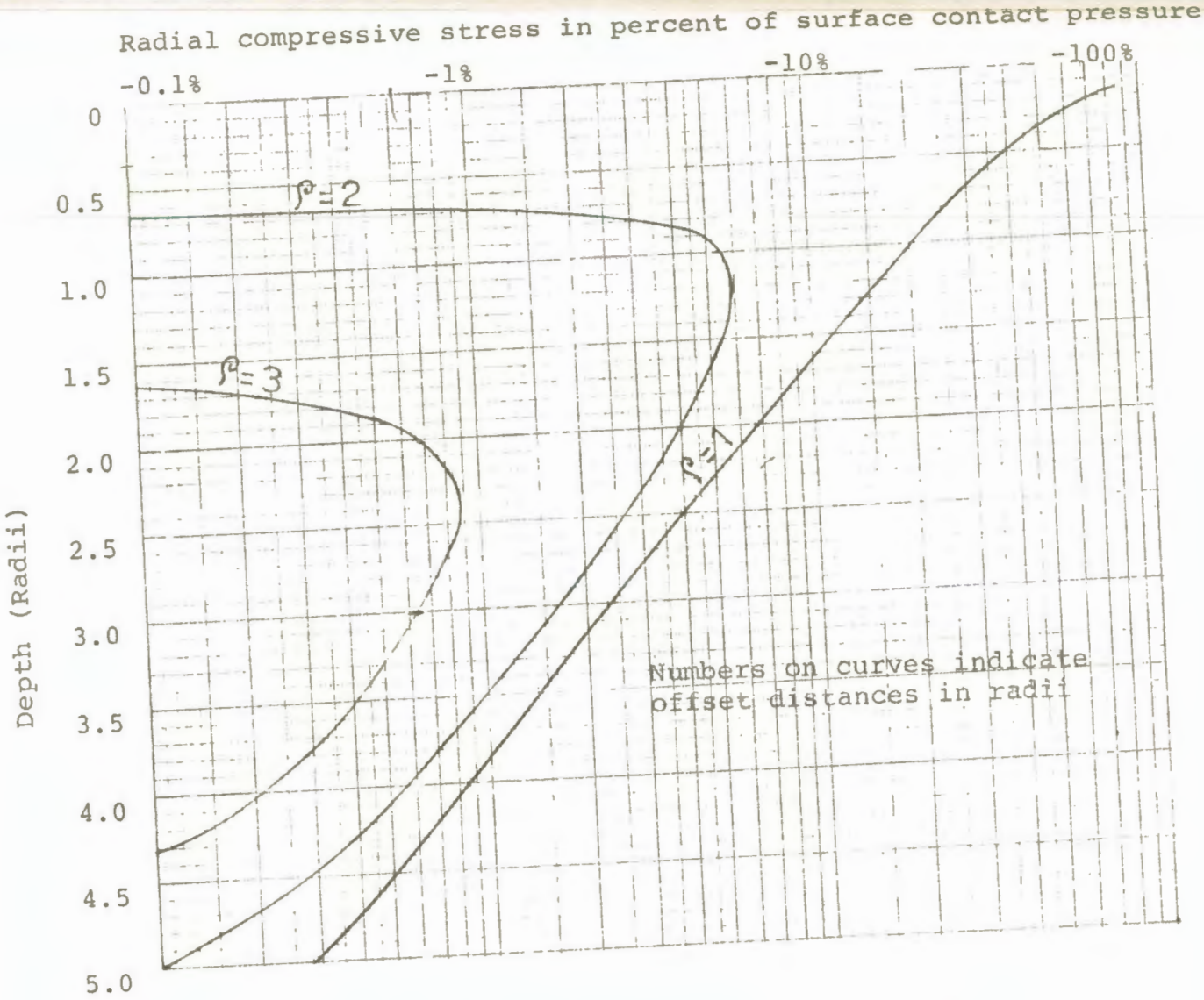

Chart 1. Radial stress (Poisson's ratio = 0.25)

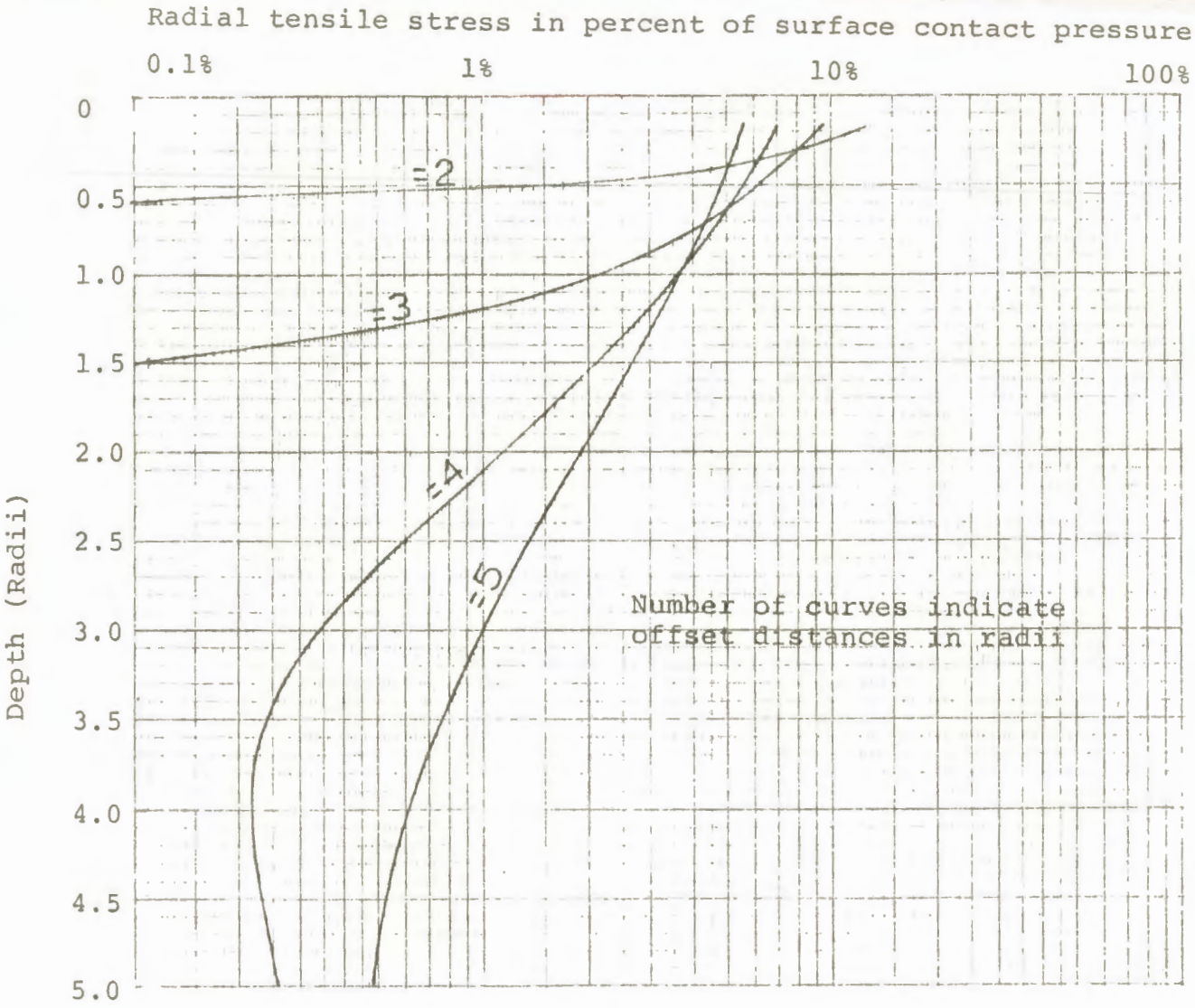

Chart 2. Radial stress (Poisson's ratio = 0.25)

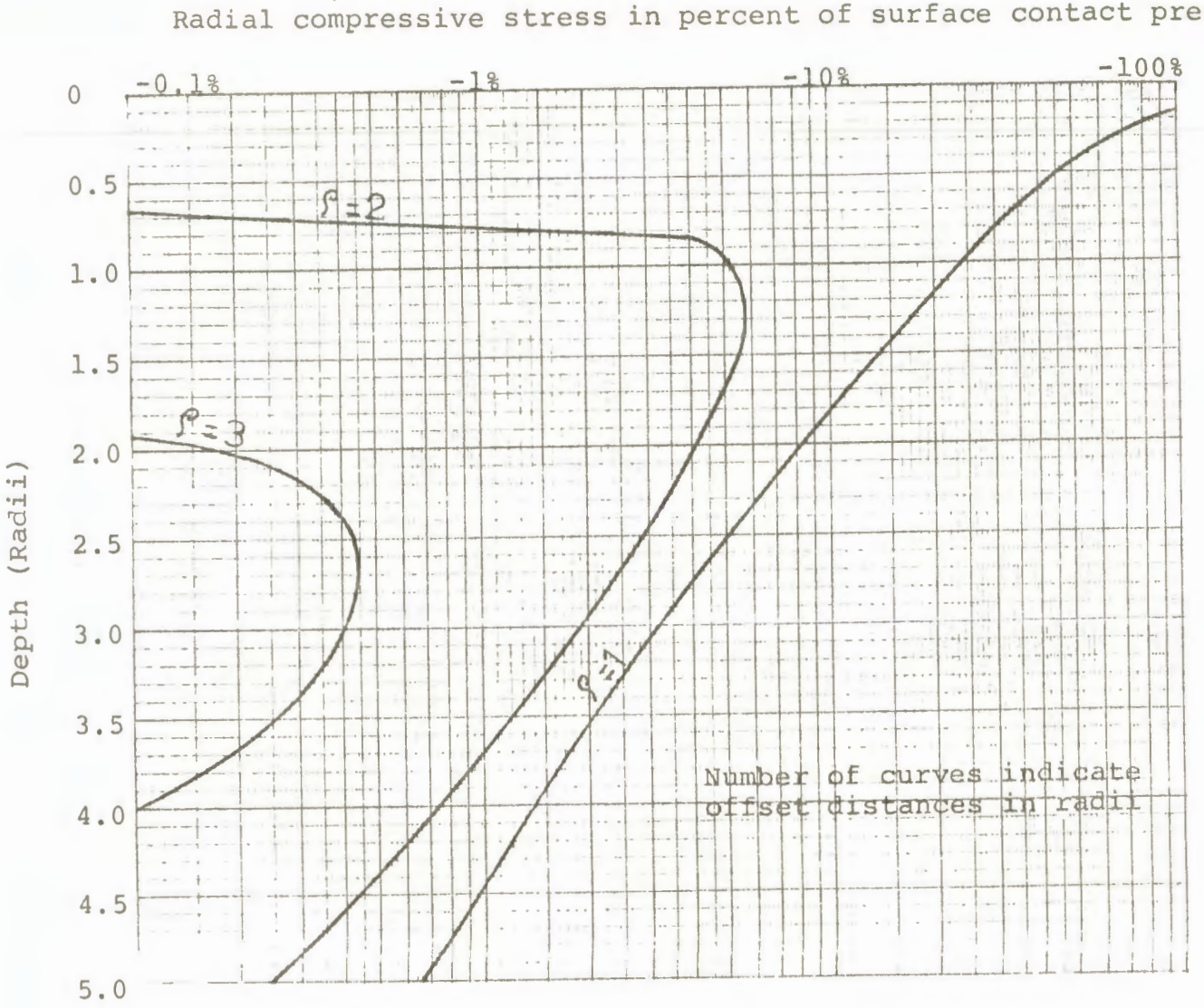

Chart 3. Radial stress (Poisson's ratio = 0.35)

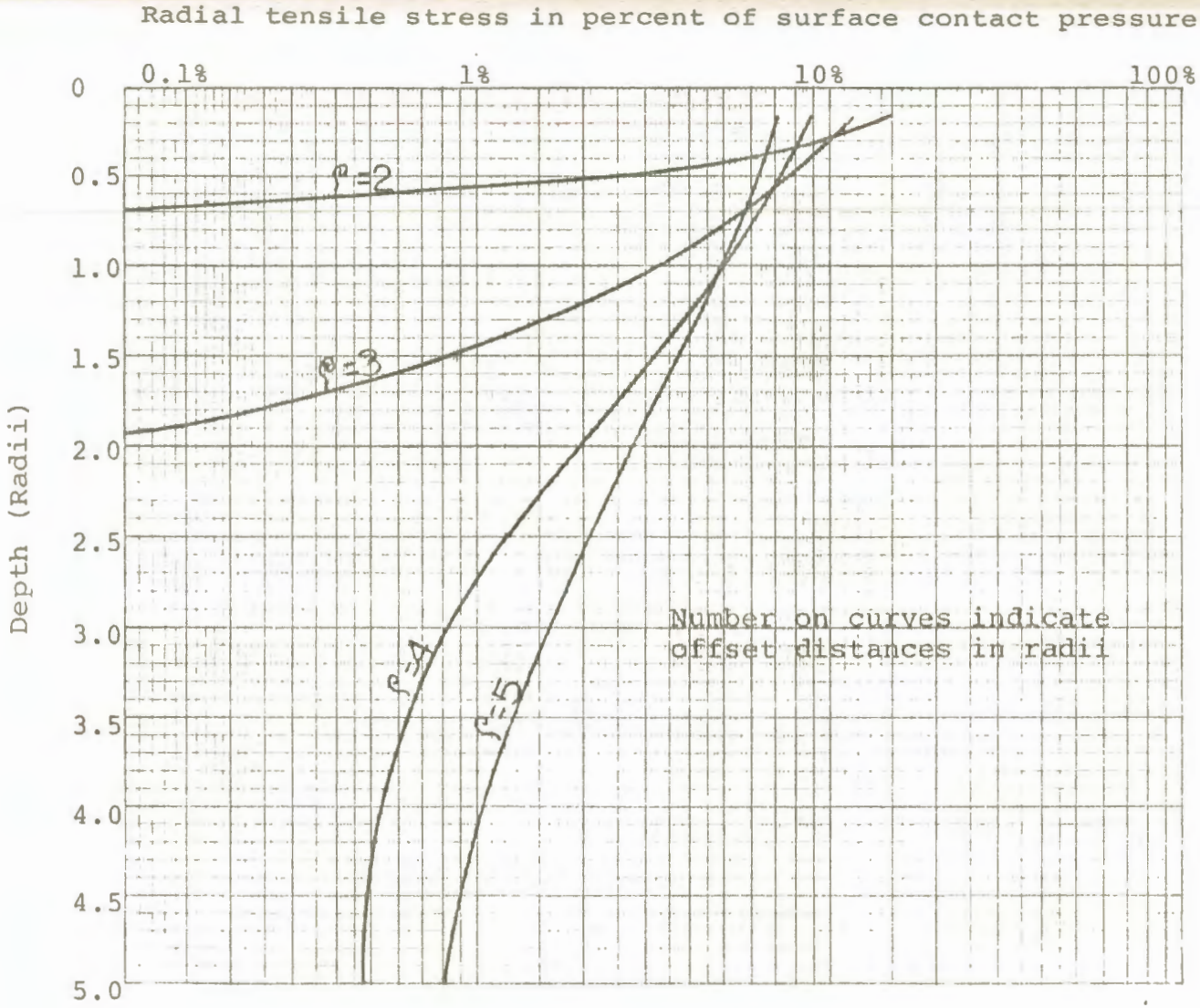

Chart 4. Radial stress (Poisson's ratio = 0.35)

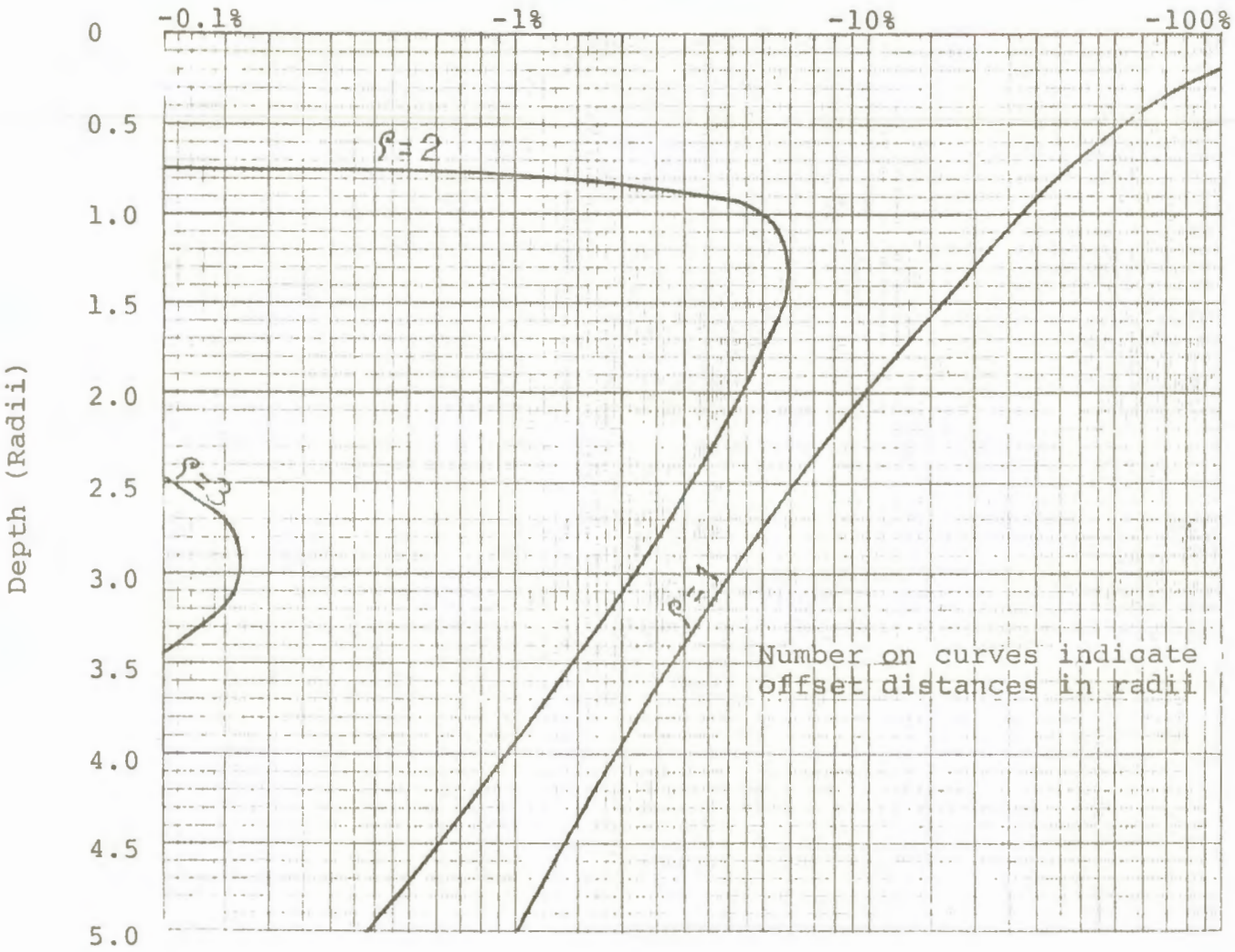

Chart 5. Radial stress (Poisson's ratio = 0.45)

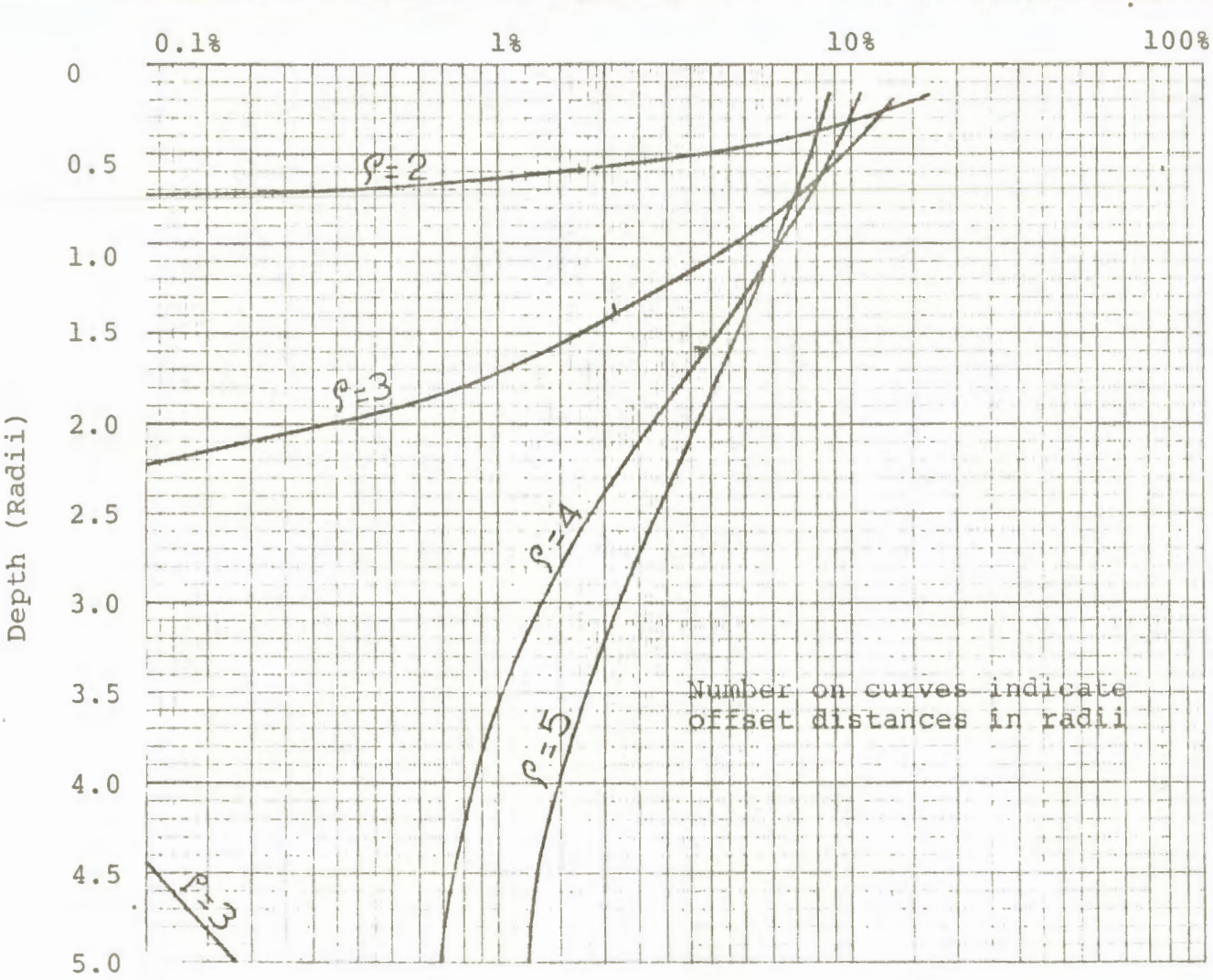

Chart 6. Radial stress (Poisson's ratio = 0.45)

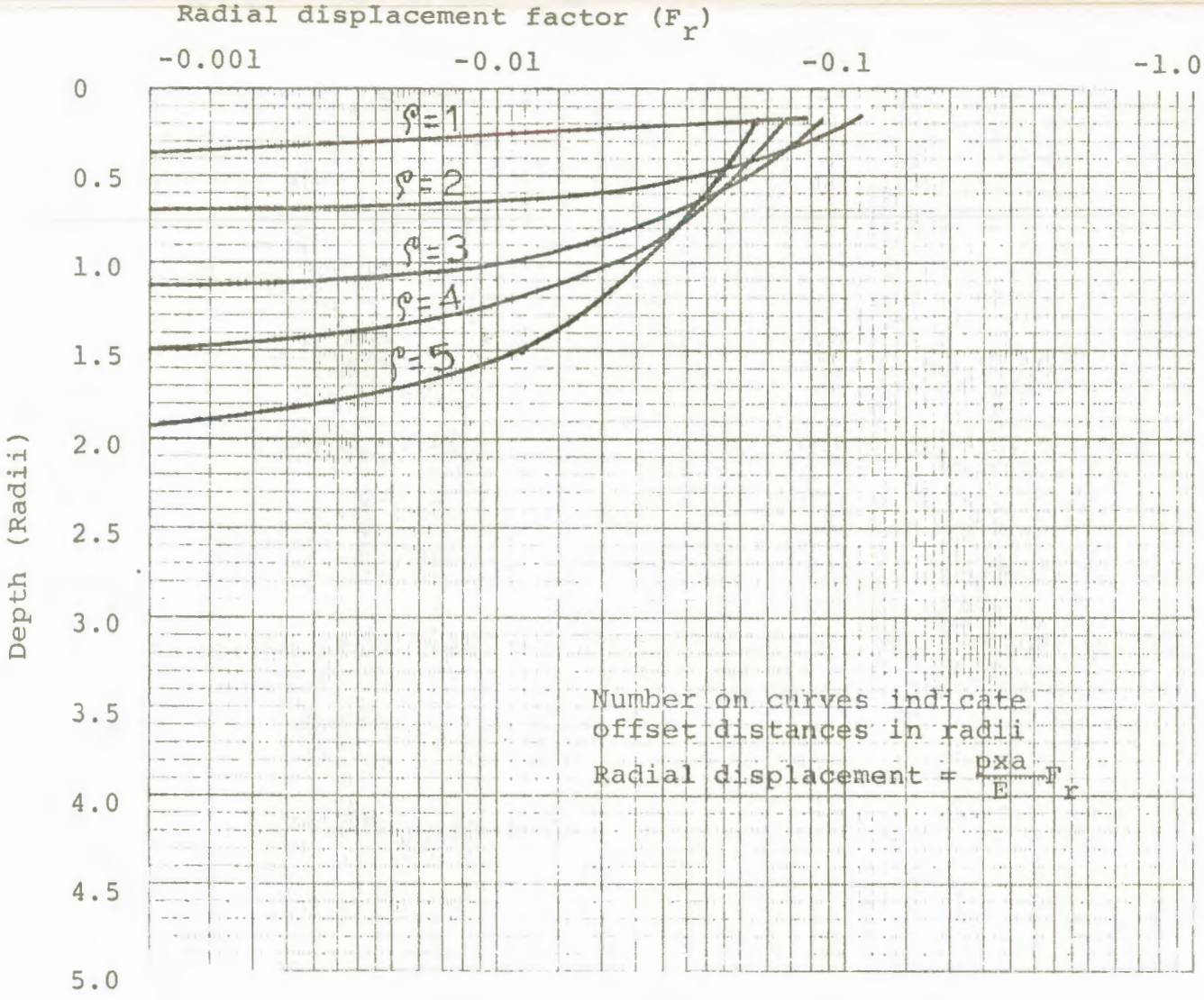

Chart 7. Radial displacement (Poisson's ratio = 0.25)

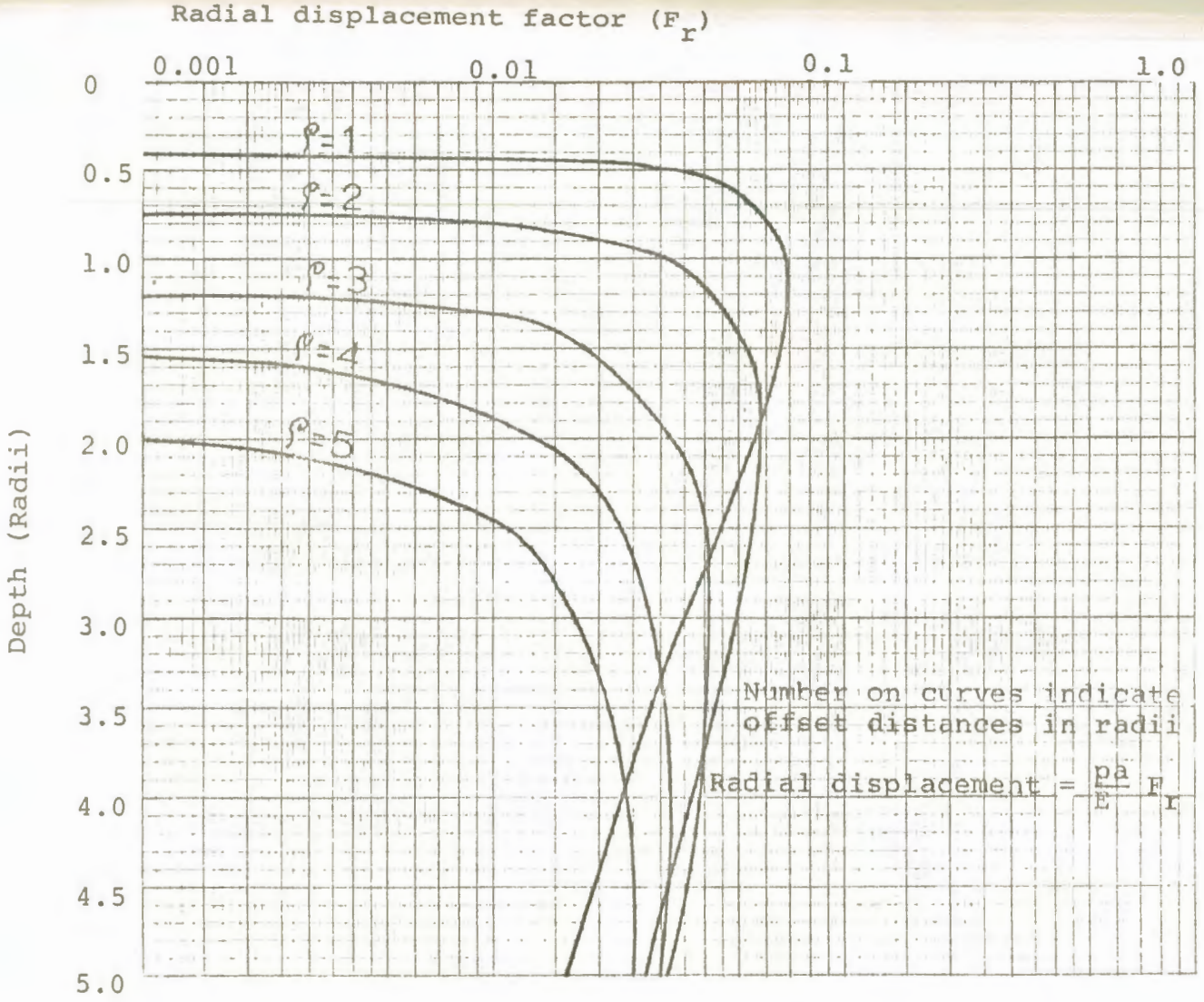

Chart 8. Radial displacement (Poisson's ratio = 0.25)

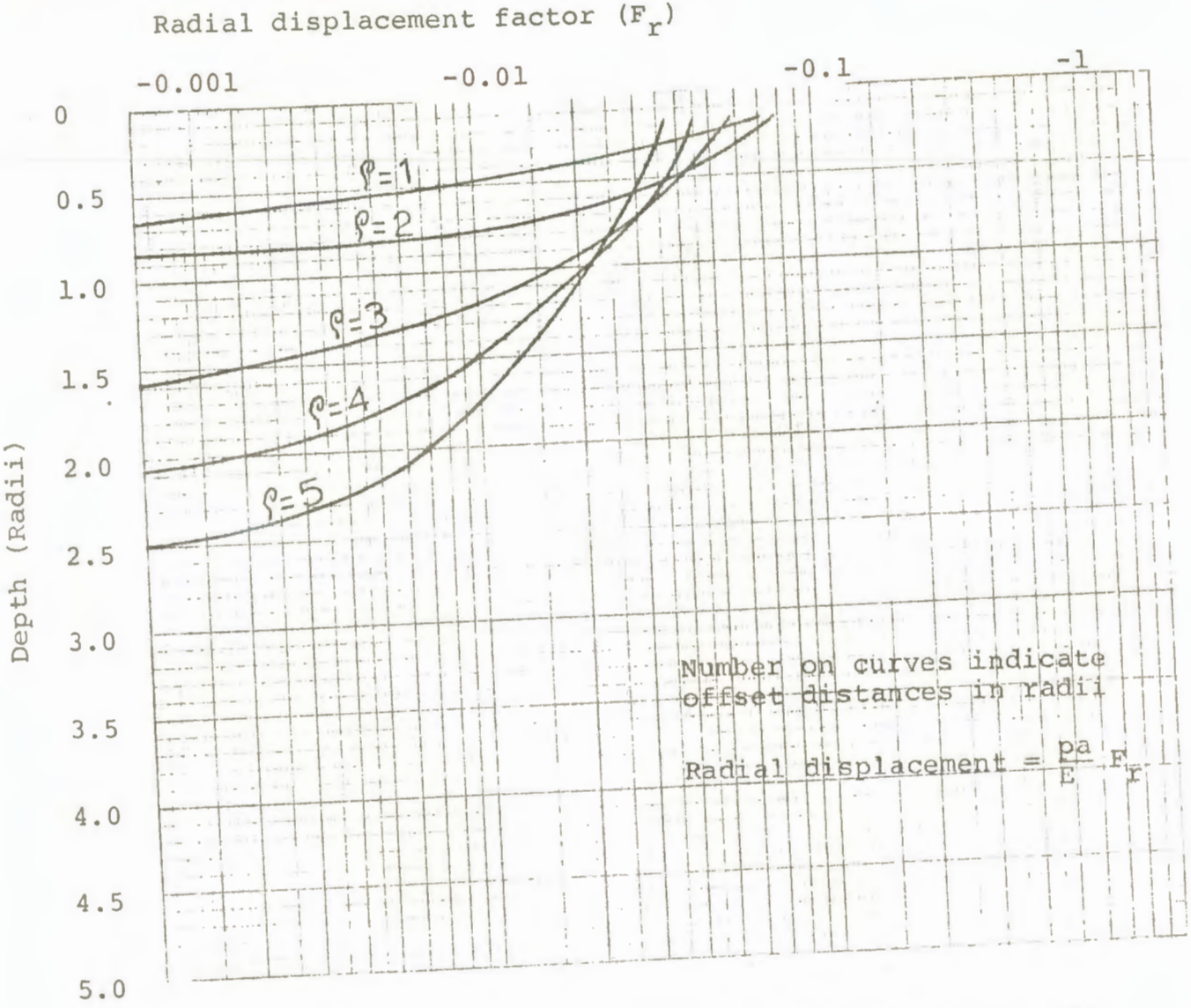

Chart 9. Radial displacement (Poisson's ratio = 0.35)

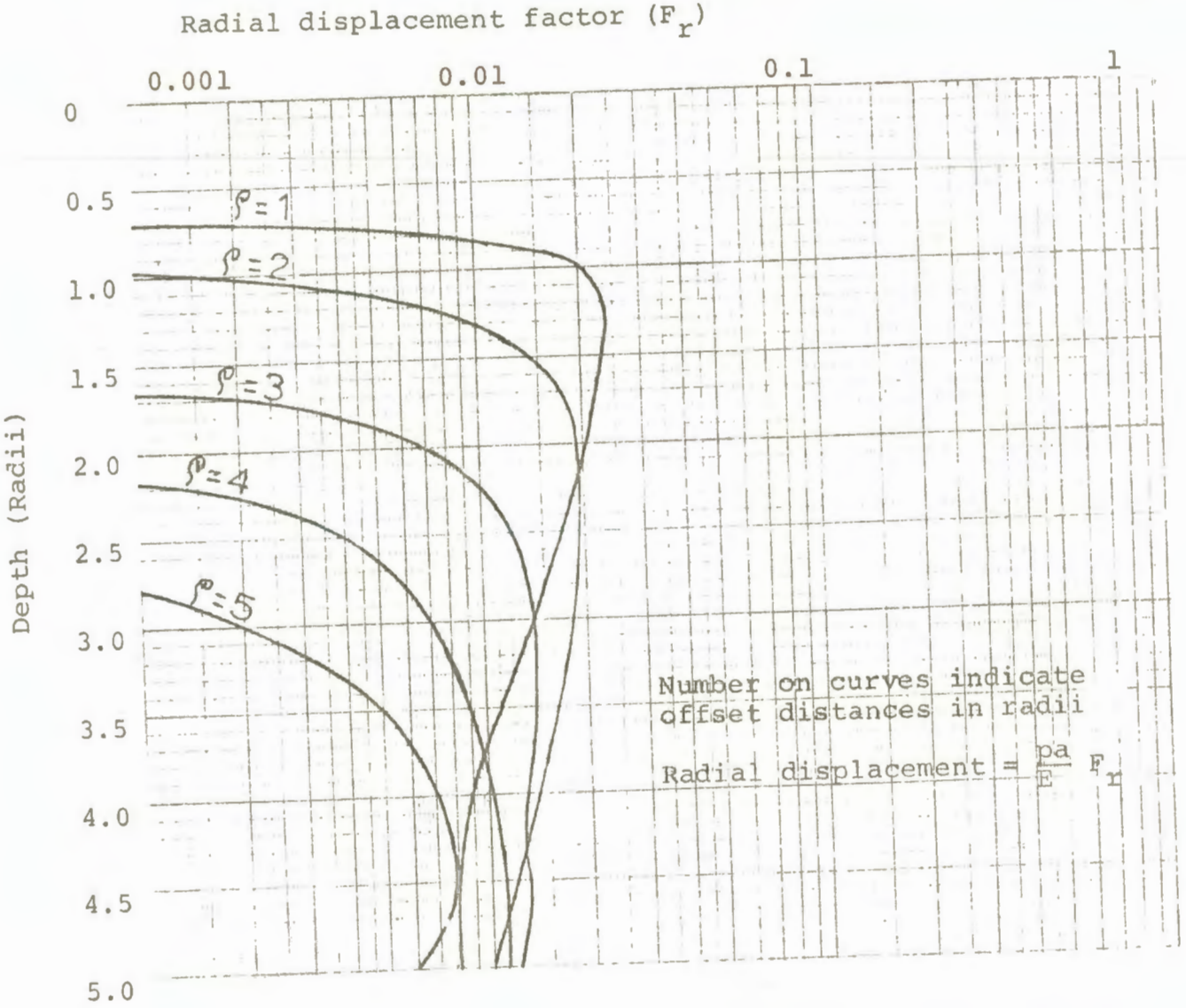

Chart 10. Radial displacement (Poisson's ratio = 0.35)

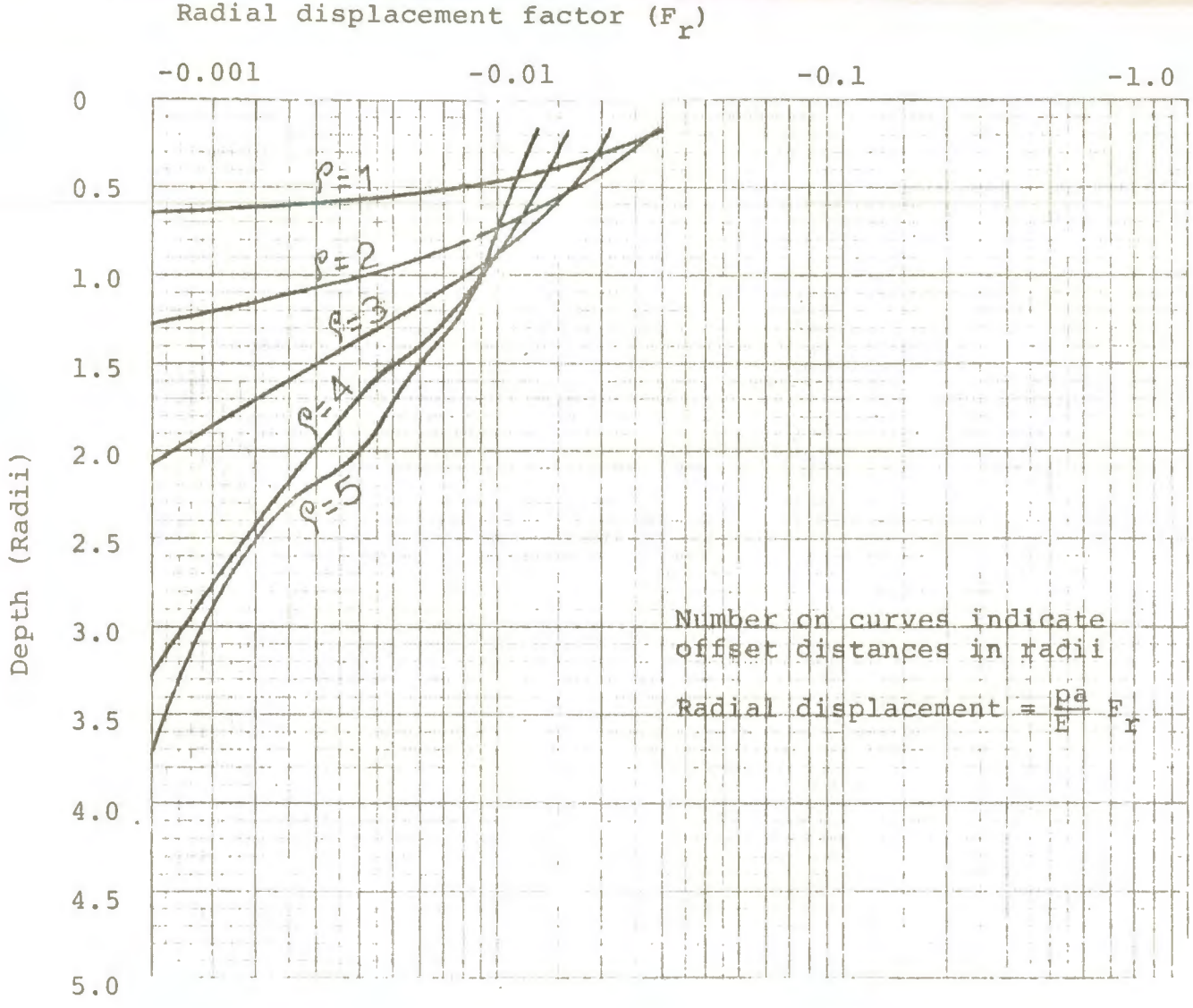

Chart 11. Radial displacement (Poisson's ratio = 0.45)

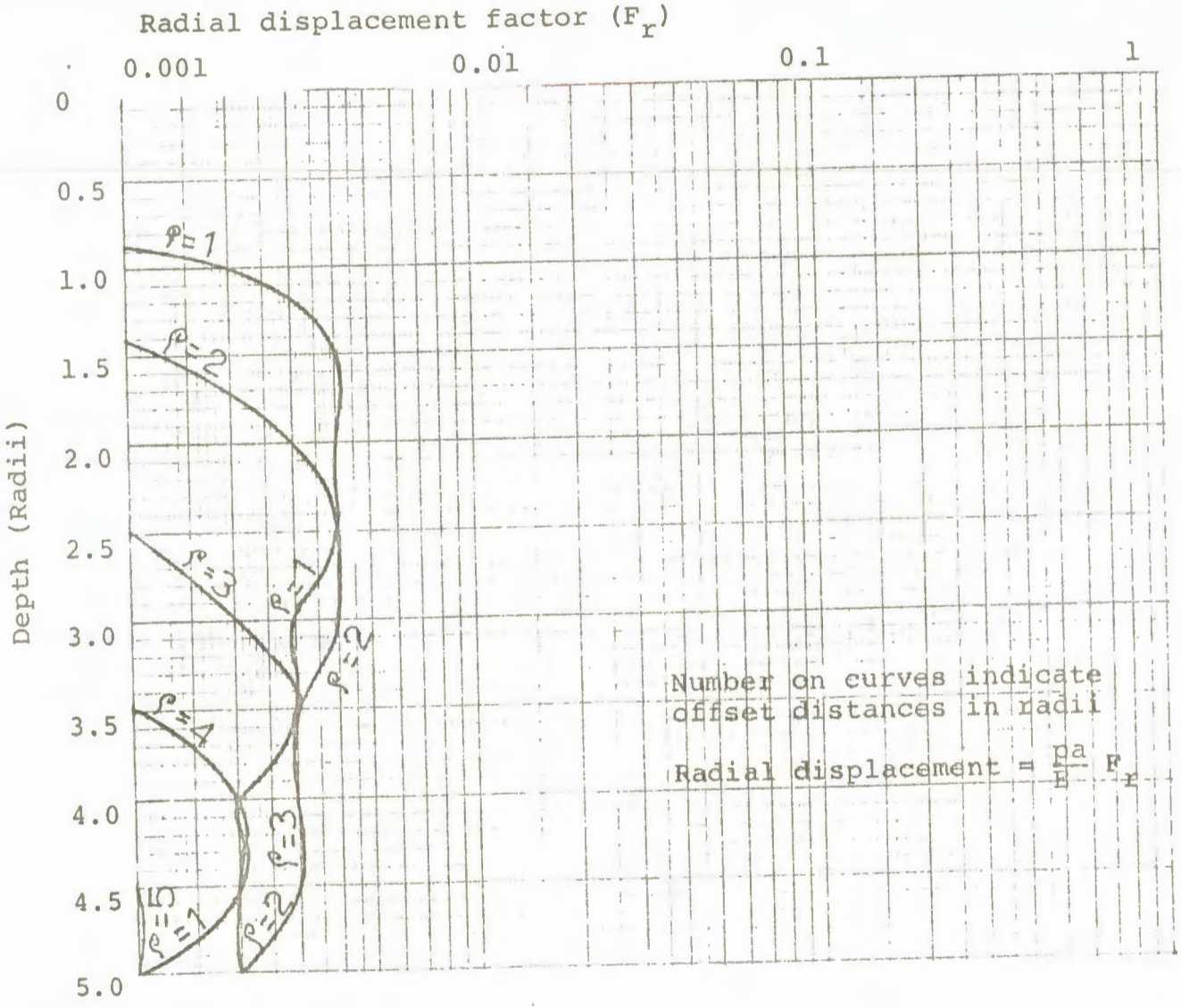

Chart 12. Radial displacement (Poisson's ratio = 0.45)

CHAPTER VI: DETERMINATION OF POISSON'S RATIO FOR THE TESTED SOIL THROUGH THE SUGGESTED METHOD

Different Steps of the Procedure

The plate bearing test was run with a 12" diameter plate, and the results of it as well as the computed modulii of elasticity that correspond to different applied vertical pressures are presented in Table 2. The general expression used to compute the soil modulii of elasticity: $E = \frac{1.5708(1 - \nu^2)}{\Delta} pa$ for a plate radius of 6" assumes the form:

$E = 7.08 \frac{p}{\Delta}$ for Poisson's ratio 0.5

$E = 7.9168 \frac{p}{\Delta}$ " " " 0.4

$E = 8.5765 \frac{p}{\Delta}$ " " " 0.3

$E = 8.8357 \frac{p}{\Delta}$ " " " 0.25

Expression (4) in Chapter V furnishes directly the radial stress as a percentage of the applied vertical pressure. Expression (5) just furnish the radial displacement factor F_r. The radial displacement was obtained through the expression: $U_r = F_r \frac{p \times a}{E}$, obtained from expression (5).

Theoretical displacements were computed for Poisson's ratios 0.3 and 0.4 and for points located within the limits given by the positions: depth equal 0.167 radii, offset distance equal 1 radii and depth equal 4 radii and offset distance equal 2.5 radii. Table 3 is a sample and presents

Table 2. Evaluation of soil modulii of elasticity for Poisson's ratios 0.25, 0.30, 0.40, and 0.50

Load (lbs.)	Pressure (p.s.i.) (p)	Deflection (in.) (Δ)	Modulii of elasticity (p.s.i.) ν=0.50 E[a]	ν=0.40 E	ν=0.30 E	ν=0.25 E
500	4.424	0.0175	17898	20.013	21681	22.336
1.000	8.849	0.0365	17165	19.193	20.792	21.421
1.500	13.274	0.057	16.487	18436	19972	20576
2.000	17.699	0.077	16273	18.197	19713	20.309
2.500	22.123	0.099	15.821	17.691	19165	19.744
3.000	26.548	0.124	15.158	16.949	18362	18.917
3.500	30.973	0.153	14.332	16.026	17.362	17.886
4.000	35.398	0.182	13.770	15.397	16.680	17.185
4.500	39.823	0.215	13.113	14.663	15.885	16.365
5.000	44.247	0.258	12.142	13.577	14.708	15.153
5.500	48.672	0.308	11.188	12.510	13.553	13.962

$$a_E = \frac{1.5708(1-\nu^2)}{\Delta} \text{ pa.}$$

Table 3. Evaluation of radial theoretical displacements for Poisson's ratio 0.3

Pressure p.s.i.	Soil modulos of elasticity p.s.i.	$\frac{pa}{E}$ in.x10^{-4}	Theoretical radial displacements (F_r= -0.080) (0.167, 1.0) in. x 10^{-4}	(F_r= -0.107) (0.167, 1.5) in. x 10^{-4}	(F_r= -0.097) (0.167, 2.0) in. x 10^{-4}	(F_r= -0.084) (0.167, 2.5)
4.424	21.681	12.243	- 0.979	- 1.310	- 1.188	- 1.028
8.849	20.792	25.536	- 2.043	- 2.732	- 2.477	- 2.145
13.274	19.972	39.878	- 3.190	- 4.267	- 3.868	- 3.350
17.699	19.713	53.870	- 4.310	- 5.764	- 5.225	- 4.525
22.123	19.165	69.260	- 5.541	- 7.411	- 6.718	- 5.818
26.548	18.362	86.749	- 6.940	- 9.282	- 8.415	- 7.287
30.973	17.362	107.037	- 8.563	-11.453	-10.383	- 8.991
35.398	16.680	127.331	-10.186	-13.624	-12.351	-10.696
39.823	15.885	150.417	-12.033	-16.095	-14.590	-12.635
44.247	14.708	180.502	-14.440	-19.314	-17.509	-15.162
48.672	13.553	215.474	-17.238	-23.056	-20.901	-18.100

The values in parenthesis give the position of the point for which the radial displacement applies. The first number gives the depth and the second the offset distance.

p = unit applied pressure

a = plate radius

E = modulus of elasticity (from Table 2)

F_r = radial displacement factor (from computer program values, or chart)

U_r = radial displacement

the values obtained for depth 0.167 radii and some offset distances.

Once the theoretical radial displacements are computed they can be translated into strain indicator readings differences (Table 4) by dividing the radial displacement, allowed theoretical displacement in Table 4, expressed in in. x 10^{-4} by 1.5238 x 10^{-4}. The result of this operation is in units of strain indicator readings, micro in./in., according to the calibration equation; piston movement vs. strain indicator reading difference (see Appendix).

The minus sign for stresses indicates compressive stresses whereas the positive sign indicates tensile stresses. Table 3 is a sample that shows the way the experimental data were recorded. The type of stresses which can be measured with the device are the compressive stresses with outward radial displacement, like those that occur at depth 2 radii and offset distances from zero to 2.5 radii; however, the device was also placed at medium positions where theoretical tensile stresses occur, like those at depth equal 0.167 radii and offset distances from zero up to 10 radii (see charts).

Experimentation

Tests were run for device's positions: depth equal 0.167 radii, offset distance equal 2.5 radii, and depth equal 2.0 radii, offset distance equal 2.5 radii. The radial theoretical displacements allowed correspond to Poisson's ratio 0.3;

Table 4. Experimental data tabulation

Vertical pressure (p.s.i.)	Allowed theoretical displacement	Strain indicator difference (through calibration)	Theoretical strain indicator (readings)	Actual strain indicator (readings)	Pressure gage reading	Horizontal stress	
						Experimental	Theoretical 12.302%
4.424	- 0.979	- 0.675	14,114.675	14.200	0.2068	0.0	0.544
8.849	- 2.043	- 1.408	14,115.408	14.220	0.2068	0.0	1.089
13.274	- 3.190	- 2.198	14,116.198	14.240	0.2068	0.0	1.633
17.699	- 4.310	- 2.969	14,116.969	14.240	0.2068	0.0	2.177
22.123	- 5.541	- 3.818	14,117.818	14.240	0.2068	0.0	2.722
26.548	- 6.940	- 4.782	14,118.782	14.200	0.2068	0.0	3.266
30.973	- 8.563	- 5.900	14,119.900	14.180	0.2068	0.0	3.810
35.398	-10.186	- 7.019	14,121.019	14.120	0.2068	0.0	4.355
39.823	-12.033	- 8.292	14,122.292	14.120	0.2068	0.0	4.899
44.247	-14.440	- 9.950	14,123.950	14.090	0.2068	0.0	5.443
48.672	-17.238	-11.878	14,125.878	14.067	0.2068	0.0	5.988

Depth = 0.167 radii

Offset distance = 2.5 radii

Contact pressure = 0.2068 p.s.i. (total in plate)

therefore the line that ties the experimental points in Figures 14 and 15 does not describe Poisson's ratio variation rigorous because step 8 of the outlined procedure has not been accomplished.

From the test data, obtained when the radial displacement was not controlled, the only one that can be used for the purpose of this procedure is the one obtained for depth equal 2 radii and offset distance equal 3 radii when no displacement was allowed. This theoretical radial displacement of zero corresponds to Poisson's ratio 0.5.

The results of these tests are presented graphically in Figures 13, 14 and 15.

For the position depth equal 2", offset distance equal 15" (Figure 13) no experimental stresses were recorded, which means that for this position the stresses were tensile or very small compressive ones. No inference can be made from this test regarding Poisson's ratio value because no experimental - theoretical comparisons are possible. The graph suggests that there is qualitative agreement between the theoretical radial stresses and the soil radial stresses for this position.

For the positions depth equal 12" offset distance equal 15" and depth equal 12" offset distance equal 18" the lines that tie together the experimental stresses do not show rigorous Poisson's ratio variation in this soil. The experimental stresses in Figure 14 correspond to displacements

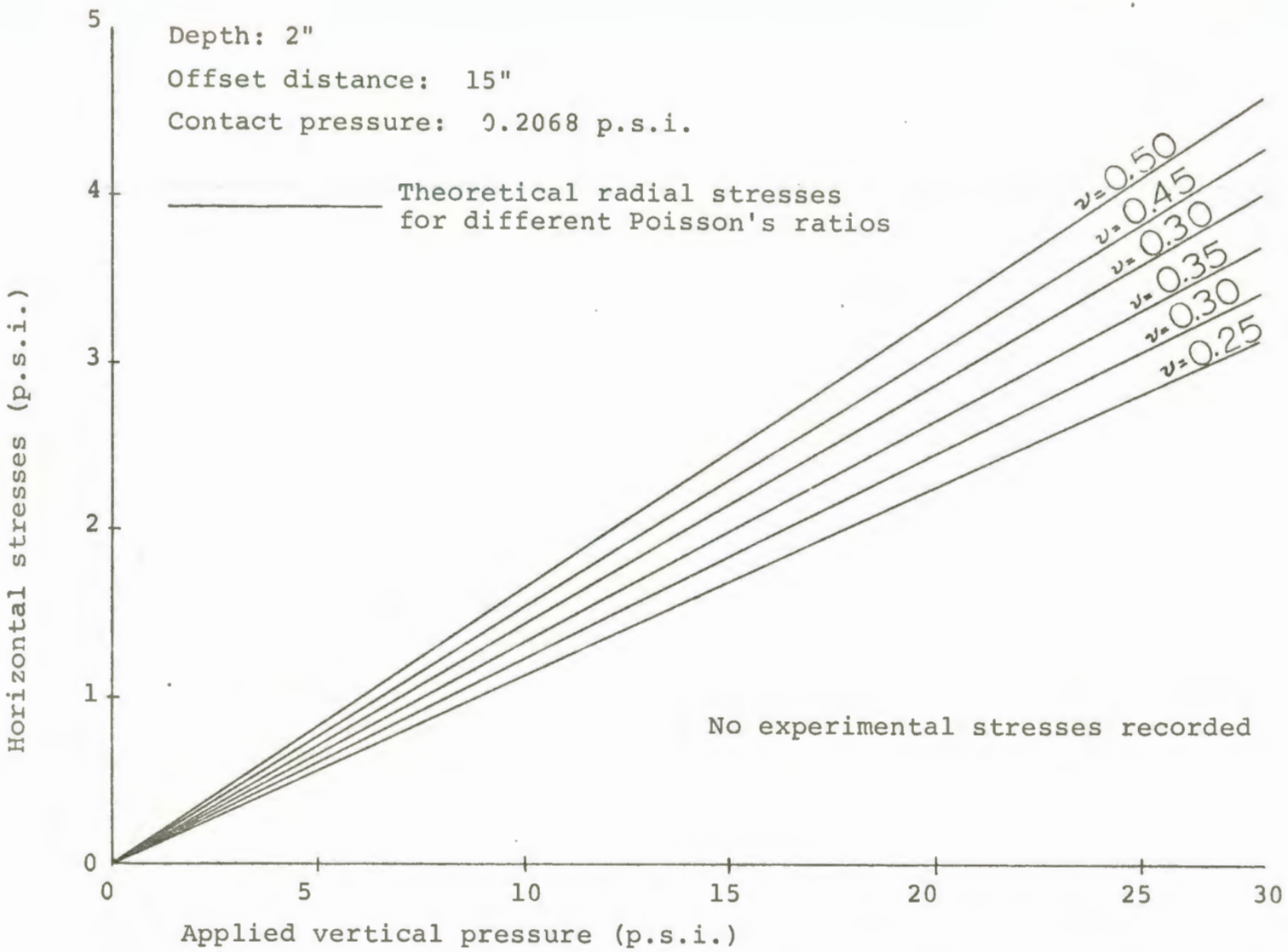

Figure 13. Recorded experimental stresses that correspond to a material whose Poisson's ratio is 0.5

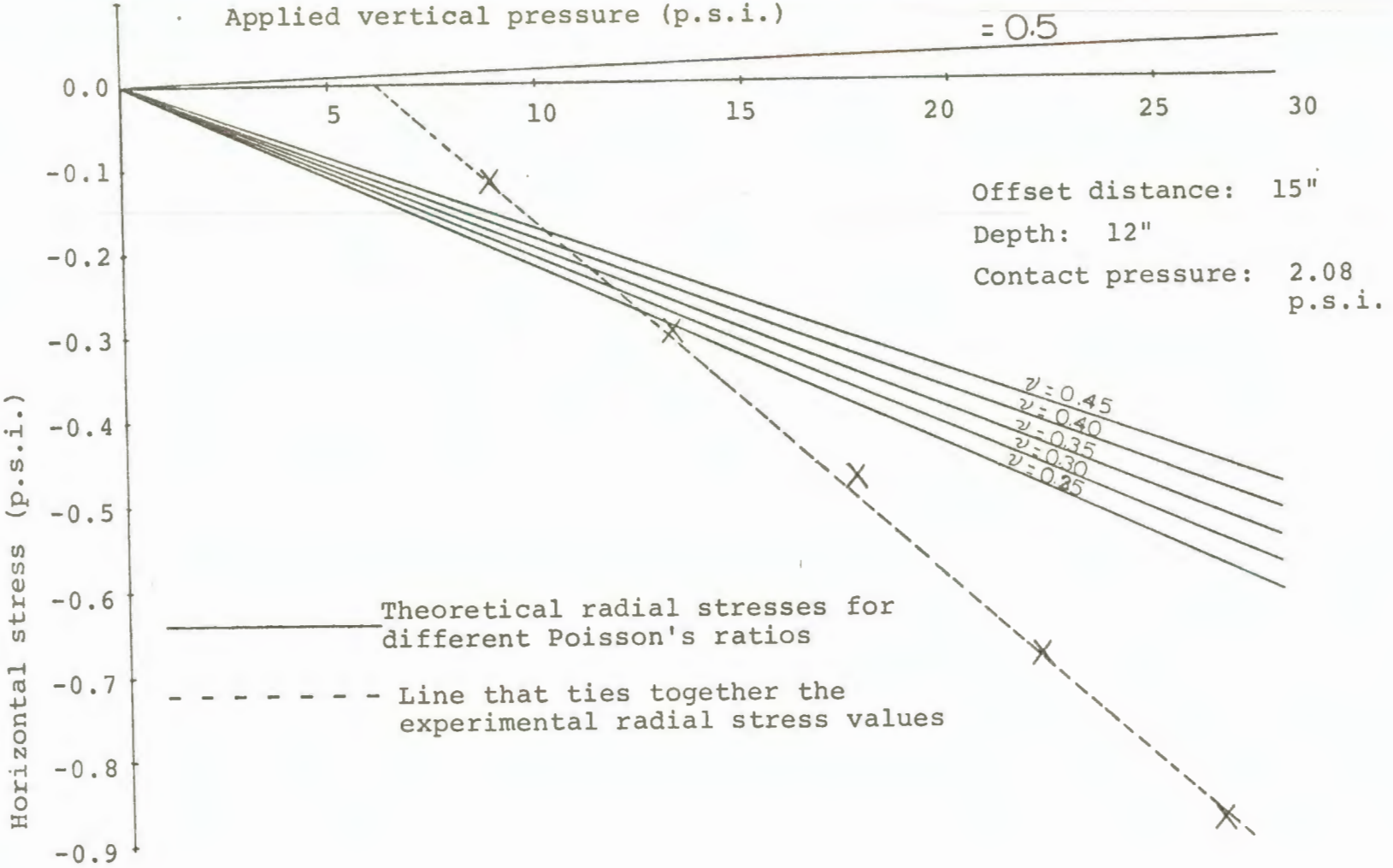

Figure 14. Recorded experimental stresses that correspond to displacements allowed by a material whose Poisson's ratio is 0.3

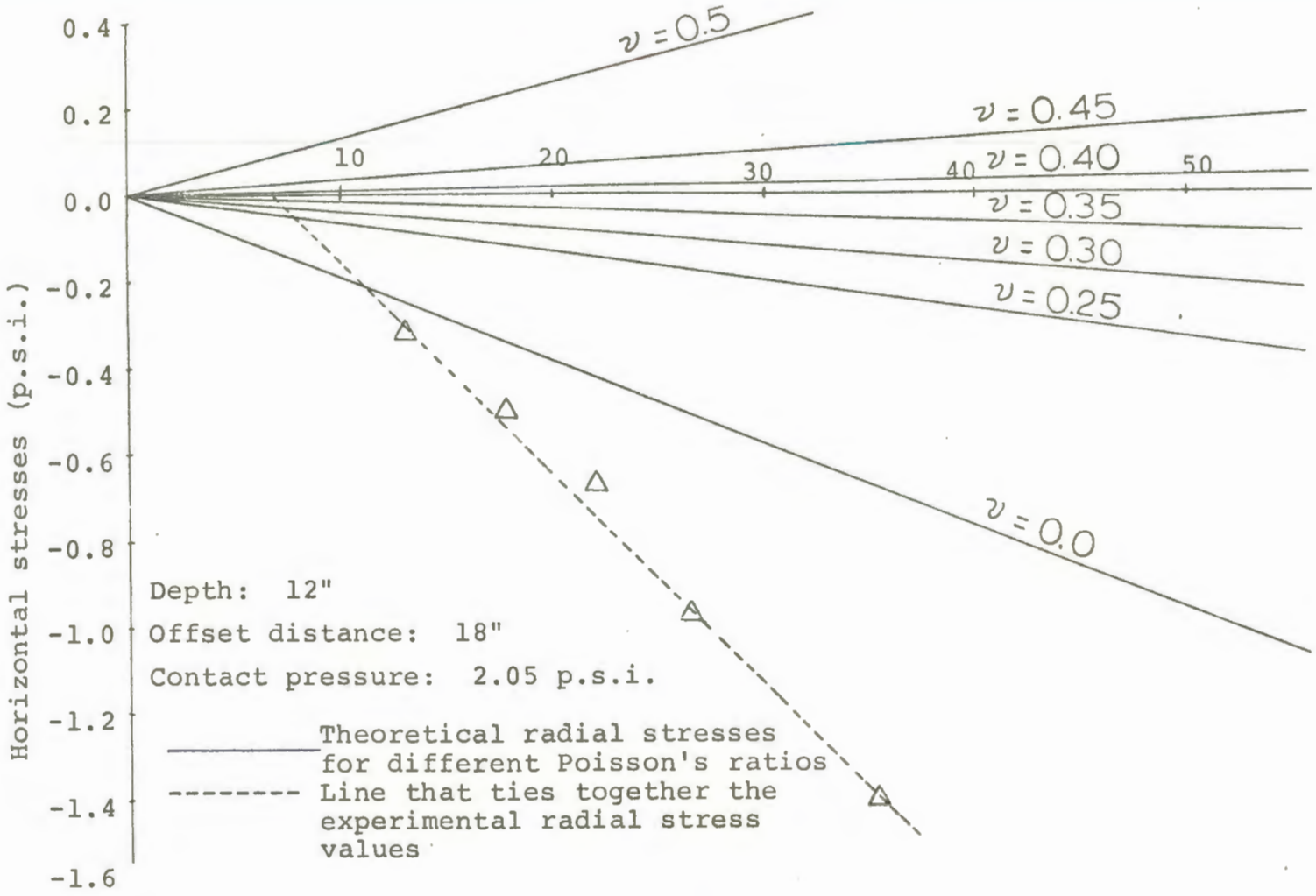

Figure 15. Recorded experimental stresses that correspond to displacements allowed by a material whose Poisson's ratio is 0.3

allowed by a material whose Poisson's ratio is 0.3, and no experimentation was carried on for displacements that correspond to material with other Poisson's ratios; therefore step 8 of the outlined procedure has not been fulfilled, and as a consequence steps 9 and 10 are not possible with the experimental data. The same reasoning applies to the experimental data in Figure 15, where the recorded experimental stresses correspond to displacements that would have been allowed by a material whose Poisson's ratio was 0.5. However, the experimental data shown in Figure 14 and 15 leave no doubt that Poisson's ratio varies because the line that ties together the experimental stresses intersects the theoretical lines.

Conclusions

1. The procedure suggested for Poisson's ratio determination in soils is reasonable; however, practical aspects of the measuring system like plate size, displacement - strain indicator difference calibration should be improved to obtain more reliable results. A good physical appreciation of the radial stress distribution has been made available through the charts, so that high radial compressive stress positions can be chosen before hand when further research is carried on.

2. A rigorous determination of Poisson's ratio for the tested soil has not been possible because the data are limited and the last steps of the suggested procedure have not been accomplished; therefore, all conclusions that follow are

acknowledged as tentative.

Experimental data conclusions

1. From Figure 14 it can be seen that for vertical pressures smaller than 6.2 p.s.i. no radial stresses were recorded, which indicates that for depth equal 2 radii offset distance equal 2.5 radii and vertical pressures smaller than 6.2 p.s.i. Poisson's ratio is about 0.5 or not computable. For depth equal 2 radii, offset distance equal 3 radii, (Figure 15) and vertical pressures smaller than 7.4 p.s.i. no soil radial stresses were recorded, so that for this position and pressures smaller than 7.4 p.s.i. Poisson's ratio may be considered between 0.5 and 0.38. However the experimental data does suggest that Poisson's ratio for this soil at the considered positions is between 0.5 and 0.3 for pressures smaller than 6 p.s.i., and varies between 0.3 and 0 for pressures between 6 p.s.i. and 12 p.s.i. Above that pressure Poisson's ratio can not be computed for this soil and position.

2. A further generalization of conclusion 1 is that Poisson's ratio decreases when the applied vertical pressure increases; therefore, for a soil mass under the influence of gravity forces (at rest condition), Poisson's ratio is larger at and near the surface than deep within the mass.

3. In most cases the pressure delivered by a structure to the soil mass is larger than about 12 p.s.i.; therefore, due to the lack of a better theory to predict stresses and displacements in soils the linear theory of elasticity may be used.

This research suggests that Poisson's ratio equal to zero should be adopted.

4. From Figures 14 and 15 it can be seen that for surcharge pressures larger than about 12 p.s.i. the compressive radial soil stresses are larger than those predicted by any linear elastic material.

5. In a linear elastic material the modulus of elasticity and Poisson's ratio remain constant regardless of the applied pressure; therefore soil can not be considered a linear elastic medium; however, since in non linear elasticity Poisson's ratio and modulus of elasticity varies, a non linear theory like the one presented by Huang (1968) may be useful.

6. Probably the reason behind the good agreement between the experimental vertical stresses and those computed through the linear elastic theory is that these computations do not require Poisson's ratio and modulus of elasticity.

7. According to Sneddon's elastic solution there are plastic zones around the edges of the plates; however, the theoretical solution does not consider the affect these plastic areas have upon the elastic stress distribution. He says that for points away from the edges, the affect of those zones is negligible. The questions faced then are: Was the device far enough away so as to consider the effect of the plastic regions negligible, or what was the quantitative effect of these plastic zones on the elastic solution for the tested positions?

BIBLIOGRAPHY

Ayres, D. J. and Hribar, J. A.
1966 General method for computing deformation in soil. Unpublished multilithed paper; abstracted from D. J. Ayres. A general method for computing stress and deformation in soils. Unpublished Ph.D. thesis. Library, Carnegie-Mellon University, Pittsburg, Pa.

Balla, A.
1960 Stress conditions in triaxial compression. Journal of the Soil Mechanics and Foundation Division 86, No. SM6: 57-84.

Burmister, D. M.
1943 Theory of stresses and displacements in layered systems and application to the design of airport runways. Highway Research Board, National Research Council Proceedings 23: 126-148.

Burmister, D. M.
1945 The general theory of stresses and displacements in layered systems. Journal of Applied Physics 16: 89.

Charyulu, Malati Kesaree.
1964 Theoretical stress distribution in an elastic multi-layered medium. Unpublished Ph.D. thesis. Library, Iowa State University, Ames, Iowa.

Coronel, Julian, Lohnes, R. A., and Handy R. L.
1968 A bore-hole device to measure lateral stresses in highway pavements. Unpublished multilithed paper presented to Iowa Highway Commission, Ames, Iowa. Dept. of Soils Engineering, I.S.U., Ames, Iowa.

Dally, James W. and Riley, William F.
1965 Experimental stress analysis. McGraw-Hill, New York, N.Y.

Dean, W. R., Parsons, H. W., and Sneddon, Ian N.
1943 A type of stress distribution on the surface of a semi-infinite elastic solid. Cambridge Philosophical Society Proceedings 40, Part 1: 5.

Foster, C. R. and Alhlvin, R. G.
1954 Stresses and deflections induced by a uniform circular load. Highway Research Board Proceedings.

Foster, C. R. and Fergus, S. M.
1951 Stress distribution in a homogeneous soil. Highway Research Board, Research Report 12F.

Harding, J. W. and Sneddon, I. N.
1944 The elastic stresses produced by the identification of the plane surface of a semi-infinite elastic solid by a rigid punch. Cambridge Philosophical Society Proceedings 41, Part 1: 16.

Ko, Hon-Yim and Scott, F. Ronald.
1968 Deformation of sand at failure. Journal of the Soil Mechanics and Foundation Division 94, No. SM4: 883-898.

Little, A. L.
1961 Foundations. Edward Arnold Ltd., London, England.

Love, A. E.
1929 The stress produce in a semi-infinite solid by pressure on part of the boundary. Royal Society Transactions, Series A: 228.

Mickle, Jack L.,
1955 Lateral pressures on retaining walls caused by uniform distributed surface loads. Unpublished M.S. thesis. Library, Iowa State University, Ames, Iowa.

Newmark, Nathan M.
1947 Influence charts for computation of vertical displacements in elastic foundations. University of Illinois Engineering Experiment Station Bulletin 367.

Newmark, Nathan M.
1942 Influence charts for computation of stresses in elastic foundations. University of Illinois Engineering Experiment Station Bulletin 338.

Obrcian, Vladimir F.
Determination of lateral pressures associated with consolidation of granular soils. Unpublished multilithed paper presented at the Highway Research Board Annual Meeting, Washington, D.C., January, 1969. Abstracted from Obrcian, V. F. A study of stress-strain and lateral pressure phenomena associated with consolidation of granular soils. Unpublished Ph.D. thesis. Microfilm Library, School of Engineering and Applied Sciences, Columbia University, New York, N.Y.

Palmer, L. A. and Barber, E. S.
1940 Soil displacement under a circular loaded area. Highway Research Board Proceedings 20: 279.

Peattie, K. R.
1963 A fundamental approach to the design of flexible pavements. International Conference on the Structural Designs of Asphalt Pavements Proceedings 1962: 403-411.

Peña, Alfonso.
1947 Mecánica elastica. Tipografia Artistica, Madrid, Spain.

Sneddon, Ian N.
1946 Boussinesq problem for a flat-ended cylinder. Cambridge Philosophical Society Proceedings 42, Part 1: 29.

Spangler, M. G. and Ustrud, H. O.
1940 Wheel load stress distribution through flexible type pavements. Highway Research Board Proceedings 20: 235.

Taylor, Donald.
1948 Fundamentals of soil mechanics. John Wiley and Sons, Inc., New York, N.Y.

Terzaghi, K. and Peck R.
1968 Soil mechanics in engineering practice. John Wiley and Sons, Inc., New York, N.Y.

Tschevotarioff, Gregory P.
1951 Mecánica del Suelo, cimientos y estructuras de tierra. Aguilar S. A. de Ediciones, Madrid, Spain.

Wang, Y. H.
1968 Stresses and displacements in non-linear soil media. Journal of the Soil Mechanics and Foundations Division 94, No. SM1: 1-19.

Westergaard, H. M.
1938 A problem of elasticity suggested by a problem in Soil Mechanics: Soft material reinforced by numerous strong horizontal sheets. Contribution to the Mechanics of Soilds dedicated to Stephen Timoshenko by his friends on the occassion of his sixteenth birthday anniversary. The Macmillan Co., New York, N.Y.

Yoder, A. J.
1959 Principles of pavement design. John Wiley and Sons, Inc., New York, N.Y.

APPENDIX

Verification of the Transformed Sneddon's Equations

Verification of the transformed Sneddon's equations (equations nos. 1, 2, 3, 4, and 5) and the computer program. The verification is given through the sequence:

1. Evaluation of Lame's elastic constants.
2. Determination of expressions equivalent to the rearranged Sneddon's equations (1), (2), (3), (4), (5), and (6).
3. Numerical evaluation of the equivalent expressions and comparisons with the numerical evaluation furnished by the computer for the transformed Sneddon's equations.

1. Evaluation of Lame's elastic constants.

It is made from the results of the plate bearing test and the elastic expressions:

$$\lambda = \frac{E\,\nu}{(1+\nu)(1-2\nu)} \qquad \mu = \frac{E}{2(1+\nu)}$$

E is obtained from the results of the plate bearing test (Table 2). Poisson's ratio = 0.4 is used for the set of computations.

Pressure p.s.i.	Modulii of elasticity	λ	μ
4.424	20.013	28.590	7.146
8.849	19.193	27.419	6.855
13.274	18.436	26.337	6.584
17.699	18.197	25.996	6.499
22.123	17.691	25.273	6.318
26.548	16.949	24.212	6.053
30.973	16.026	22.894	5.724
35.398	15.397	21.996	5.499
39.823	14.663	20.947	5.237
44.247	13.577	19.396	4.849
48.672	12.510	17.871	4.468

2. Determination of expressions equivalent to the rearranged Sneddon's equations.

This is possible through the equation:

$$\frac{\Delta}{a} = \frac{1 - \nu^2}{2} \frac{p}{E}$$

obtained from the already used equality:

$$p(\pi a^2) = \frac{2}{1 - \nu^2} E\Delta a$$

Once this replacement is performed, the following expressions equivalent to the transformed Sneddon's equations are obtained:

$$100 \frac{\sigma_z}{p} = -200 \frac{(\lambda+\mu)}{\lambda+2\mu} \frac{(1-\nu^2)}{E} (J_1^0 + \zeta J_2^0) \qquad (1)'$$

$$100 \frac{T_{2r}}{p} = -200 \frac{\mu(\lambda+\mu)}{\lambda+2\mu} \frac{1-\nu^2}{E} \zeta J_2^1 \qquad (2)'$$

$$100 \frac{\sigma_\theta}{p} = -200 \frac{1-\nu^2}{E} [\frac{\lambda\mu}{\lambda+2\mu} J_0^1 + \frac{\mu^2}{\zeta(\lambda+2\mu)} (J_0^1 - \frac{\lambda+\mu}{\mu} \zeta J_2^1) \qquad (3)'$$

$$100 \frac{\sigma_r}{p} = -200 \frac{1-\nu^2}{E} \{\frac{\mu}{\lambda+2\mu}[(2\lambda+\mu)J_1^0 - (\lambda+\mu) J_2^0] - \frac{\lambda\mu}{\lambda+2\mu} J_0^1$$

$$- \frac{\mu^2}{\zeta(\lambda+2\mu)} (J_0^1 - \frac{\lambda+\mu}{\mu} \zeta J_2^1)\} \qquad (4)'$$

$$\frac{E}{pa} U_r = - \frac{\mu}{\lambda+2\mu} (1-\nu^2)(J_0^1 - \frac{\lambda+\mu}{\lambda} \zeta J_1^1) \qquad (5)'$$

$$\frac{E}{pa} U_v = (1-\nu^2)(J_0^0 + \frac{\lambda+\mu}{\lambda+2\mu} \zeta J_1^0) \qquad (6)'$$

3. Numerical evaluation of the equivalent expressions (1)', (2)', (3)', (4)', and (5)' and comparison with:

1. Evaluation of Lame's elastic constants.

2. Determination of expressions equivalent to the rearranged Sneddon's equations (1), (2), (3), (4), (5), and (6).

3. Numerical evaluation of the equivalent expressions and comparisons with the numerical evaluation furnished by the computer for the transformed Sneddon's equations.

The evaluation is made for the position:

Depth = $\zeta = \frac{1}{6}$ radii = 0.167 radii

Offset distance = ρ = 1 radii

The values used for E, λ and μ correspond to the pressure 4.424 p.s.i.

$$r^2 = 1 + \frac{1}{6^2} = \frac{37}{36} \qquad \therefore \quad r = 1.0137938$$

$$R^2 = \left(1 + \frac{1}{36} - 1\right)^2 + 4 \times \frac{1}{36} = \frac{145}{36^2} \qquad \therefore \quad R = 0.3344886$$

$$\tan \theta = \frac{1}{\frac{1}{6}} = 6 \qquad \therefore \quad \theta = 80^\circ\ 32'\ 15.6"$$

$$\tan \phi = \frac{2 \times \frac{1}{6}}{\frac{1}{36}} = 12 \qquad \therefore \quad \phi = 85^\circ\ 14'\ 11.2"$$

$$J_1^0 = \frac{\sin 42^\circ\ 37'\ 5.6"}{\sqrt{0.3344886}} = 1.17059$$

$$J_2^0 = \frac{1.0137938 \times \sin 7^\circ\ 04'\ 23.4''}{0.3344886\ \sqrt{0.3344886}} = 0.64534$$

$$J_0^1 = \frac{1}{1}\ (1 - \sqrt{0.3344886}\ \sin 42^\circ\ 37'\ 57.6'') = 0.60849$$

$$J_1^1 = \frac{1.0137938 \sin 38^\circ\ 55'\ 10''}{1\ \sqrt{0.3344886}} = 1.10132$$

$$J_2^1 = \frac{\sin 127^\circ\ 51'\ 16.8''}{1 \times 0.3344886 \sqrt{0.3344886}} = 4.08194$$

4. Numerical evaluation of expressions (1)', (2)', (3)', (4)', and (5)':

$$100\ \frac{\sigma_2}{p} = -200\ \frac{7,146 \times 35,736}{42,882} \times \frac{0.84}{20.013}\ (1,170.59 + \frac{1}{6} \times 0.64534)$$

$$100\ \frac{\sigma_2}{p} = -\ 63.868\%;\ 100\ \frac{\sigma_2}{p}\ \text{computer} = -63.838\%$$

$$100\ \frac{T_{2r}}{p} = \frac{7,146 \times 35,736 \times 168}{42,882 \times 20,013} \times \frac{4.08194}{6}$$

$$100\ \frac{T_{2r}}{p} = -\ 34.0102\%;\quad 100\ \frac{T_{2r}}{p}\ \text{computer} = -33.984\%$$

$$100\ \frac{\sigma_\theta}{p} = -200\ \frac{0.84}{20,013}\ [\frac{28,590 \times 7,146}{42,882} \times 0.60849 +$$

$$+ \frac{7,146^2}{42,882}\ (0.60849 - \frac{35,736}{7,146} \times \frac{1}{6} \times 4,08194)]$$

$$100\ \frac{\sigma_\theta}{p} = 3.5909\% \qquad 100\ \frac{\sigma_0}{p}\ \text{computer} = 3.583\%$$

$$100\ \frac{\sigma_r}{p} = -200\ \frac{0.84}{20{,}013}\ \{[\frac{7{,}146}{42{,}882}\ [64{,}326 \times 1.1705 - 35{,}736 \times \frac{1}{6} \times 0.64534]$$

$$- \frac{28{,}590 \times 7{,}146}{42{,}882} \times 0{,}60849 - \frac{7{,}146^2}{42{,}882}\ (0.60849 - \frac{35{,}736}{7{,}146} \times \frac{1}{6}$$

$$\times\ 4{,}08194)\}$$

$$100\ \frac{\sigma_r}{p} = -103.547\% \qquad 100\ \frac{\sigma_r}{p}\ \text{computer} = -103.472\%$$

$$\frac{E}{pa}\ U_r = -\ \frac{7{,}146}{42{,}882} \times 0.84\ (0.60849 - \frac{35{,}736}{28{,}590} \times \frac{1}{6} \times 1.10132)$$

$$\frac{E}{pa}\ U_r = -\ 0.0530599 \qquad \frac{E}{pa}\ U_r\ \text{computer} = 0.054$$

Calibration

Piston displacement -- strain indicator readings are seen in Figure 16.

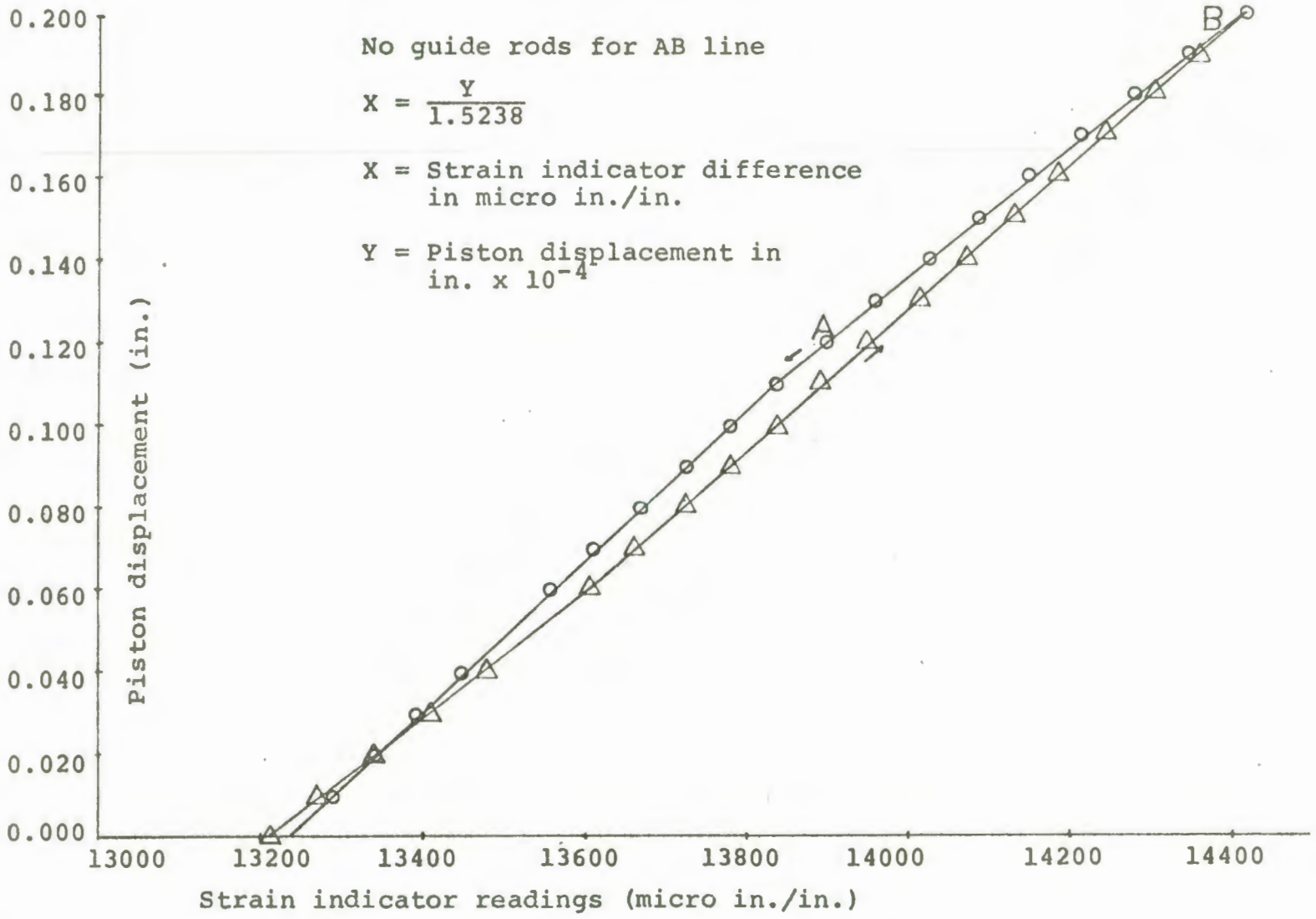

Figure 16. Piston displacement vs. strain indicator readings

Computer Program

```
      IT IS DESIGNED TO ENABLE THE USER TO EXPERIMENT WITH VAR-
      IOUS COMBINATIONS OF DEPTH, OFFSET DISTANCE, AND POISSON'S
      RATIO.
      DEPTH=S, RHO=OFFSET, (BOTH IN RADII),U=POISSON'S RATIO
      DIMENSION U(10),RHO(20),NAME(10)
      INTEGER DATE
      USER NAMES ARE ON THE FIRST DATA CARD
      N=#OF RHO'S, L=# OF U'S, DATE IS ALSO READ IN ON 2ND DATA
      CARD
      READ(1,1)(NAME(I),I=1,10)
    1 FORMAT(10A4)
      READ(1,2)DATE,N,L
    2 FORMAT(16,13,13)
      PUNCH ALL VALUES OF U ON ONE CARD IN THE FORM XX.XXXX.XX...
      READ(1,3)(U(K),K=1,L)
    3 FORMAT(10F5.2)
      PUNCH EACH VALUE OF RHO ON A SEPARATE CARD, XX.XXX
      READ(1,4)(RHO(J),J=1,N)
    4 FORMAT(F6.3)
      WRITE(3,5)DATE,(NAME(I),I=1,10)
    5 FORMAT('IISU SOILS ENGINEERING LABORATORY',10X,'DATE:',16,'
      RESULTS L FOR:',10A4)
      WRITE(3,6)
    6 FORMAT('OSCLUTION OF BOUSSINESQ PROBLEM FOR A FLAT ENDED
      CYLINDER' 1,20X, 'OUTPUT VARIABLES ARE DEFINED AS FOLLOWS:')
      WRITE(3,7)
    7 FORMAT('CS=DEPTH, RHO=OFFSET, U=POISSON'S RATIO, P=TEST
      PRESSURE, lA=PLATE RADIUS, E=MODULUS OF ELASTICITY')
      WRITE(3,8)
    8 FORMAT('F1=100SIGMA(Z)/P, F2=100TAU(ZR)/R, F3=100SIGMA
      (THETA)/P, LF4=100SIGMA(RADIAL/P, F5=EU(R)/PA')
      WRITE(3,9)
    9 FORMAT('ODATA USED IN COMPUTATIONS:')
      WRITE(3,22)
   22 FORMAT('ORHO:')
      WRITE(3,10)(RHO(J),J=1,K)
   10 FORMAT(F8.3)
      WRITE(3,11)
   11 FORMAT('OU:')
      WRITE(3,12)(U(K),K=1,L)
   12 FORMAT(F8.2)
      EACH S IS PUNCHED ON A SEPARATE CARD (XX.XXX),LAST S=999999
  100 READ(1,13)S
   13 FORMAT(F6.3)
      WRITE(3,14)S
   14 FORMAT('IS=',F8.3)
      IF(S-100) 101,104,104
```

```
101 R2=(1.0+S**2.0)
    WRITE(3,15)
 15 FORMAT('0',4X,'RHO',7X,'F1',7X'F2',8X'U',9X,'F3',8X,'F4',
    8X,'F5'1)
    Z1=1.C/S
    THETA=ATAN(Z1)
    R=SQRT(R2)
    J=1
    DO 103 J=1,N
    Z2=((RHO(J)**2.0)+R2-2.0)
    RR2=(Z2*Z2)+(4.0*S**2.0)
    ZFE=2.0*S/Z2
    FE=ATAN(ZFE)
    RR=SQRT(RR2)
    FE2=FE/2.0
    SFE2-SIN(FE2)
    ZJ10=(RR**(-0.5))*SFE2
    ZJ01=(1.0/RHO(J))*(1.0-((RR**0.5)*SFE2))
    FE32=1.5*FE
    SFE32=SIN(FE32)
    ZJ21=(RHO(J)*(RR**(-1.5)))*SFE32
    FETH1=(FE-THETA)*1.5
    SFETH=SIN(FETH1)
    ZJ20=R*(RR**(-1.5))*SFETH
    FETH2=(THETA-FE2)
    SFETH=SIN(FETH2)
    ZJ11=(R/RHO(J))*((RR**(-0.5))*SFETH)
    F1=-50.0*(ZJ10+S*ZJ20)
    F2=-50.0*S*ZJ21
    WRITE(3,16)RHO(J),F1,F2
 16 FORMAT('',F7.2,F10.3,F9.3)
    K=1
    DO 102 K=1,L
    IF(U(K)-0.5)105,106,105
106 F3=-100.0*U(K)*ZJ01
    F4=-50.0*((2.0*U(K)+1.0)*ZJ10-(S*ZJ20))+100.0*U(K)*ZJ01
    GO TO 107
105 F3=-100.0*U(K)*ZJ01-50.0/RHO(J)*(1.0-2.0*U(K))*(ZJ01-
    (S*ZJ21)/(1.0 1-2.0*U(K)))
    F4=-50.0*((2.0*U(K)+1.0)*ZJ10-(S*ZJ20))+100.0*U(K)*ZJ01
    +50.0/RHO(J 1)*(1.0-2*U(K))*ZJ01-(S*ZJ21)/(1.0-2.0*U(K)))
107 F5=-(1.0-U(K)-2.0*U(K)**2.0)*0.5*(ZJ01-0.5*S*ZJ11/U(K)))
102 WRITE(3,17)U(K),F3,F4,F5
 17 FORMAT('',27X,F9.2,F11.3,F10.3,F10.3)
103 CONTINUE
    GO TO 100
104 WRITE(3,18)
    STOP
    END
```